Title

Caenorhabditis elegans polo-like kinase PLK-1 is required for merging parental genomes into a single nucleus

Journal

Molecular Biology of the Cell, 26(25)

ISSN

1059-1524

Authors

Rahman, Mohammad M
Munzig, Mandy
Kaneshiro, Kiyomi
et al.

Publication Date

2015-12-15

DOI

10.1091/mbc.e15-04-0244

Peer reviewed

Caenorhabditis elegans polo-like kinase PLK-1 is required for merging parental genomes into a single nucleus

Mohammad M. Rahman[a], Mandy Munzig[b], Kiyomi Kaneshiro[c], Brandon Lee[a], Susan Strome[c], Thomas Müller-Reichert[b], and Orna Cohen-Fix[a]

[a]Laboratory of Cell and Molecular Biology, National Institute of Diabetes and Digestive and Kidney Diseases, National Institutes of Health, Bethesda, MD 20892; [b]Structural Cell Biology Group, Experimental Center, Medical Faculty Carl Gustav Carus, University of Technology Dresden, 01307 Dresden, Germany; [c]Department of Molecular, Cell and Developmental Biology, University of California, Santa Cruz, Santa Cruz, CA 95064

ABSTRACT **Before the first zygotic division, the nuclear envelopes of the maternal and paternal pronuclei disassemble, allowing both sets of chromosomes to be incorporated into a single nucleus in daughter cells after mitosis. We found that in *Caenorhabditis elegans*, partial inactivation of the polo-like kinase PLK-1 causes the formation of two nuclei, containing either the maternal or paternal chromosomes, in each daughter cell. These two nuclei gave rise to paired nuclei in all subsequent cell divisions. The paired-nuclei phenotype was caused by a defect in forming a gap in the nuclear envelopes at the interface between the two pronuclei during the first mitotic division. This was accompanied by defects in chromosome congression and alignment of the maternal and paternal metaphase plates relative to each other. Perturbing chromosome congression by other means also resulted in failure to disassemble the nuclear envelope between the two pronuclei. Our data further show that PLK-1 is needed for nuclear envelope breakdown during early embryogenesis. We propose that during the first zygotic division, PLK-1–dependent chromosome congression and metaphase plate alignment are necessary for the disassembly of the nuclear envelope between the two pronuclei, ultimately allowing intermingling of the maternal and paternal chromosomes.**

Monitoring Editor
Yixian Zheng
Carnegie Institution

Received: Apr 24, 2015
Revised: Oct 7, 2015
Accepted: Oct 13, 2015

INTRODUCTION

After fertilization, chromosomes contributed by the two parents are intermingled to generate the genetic material of the offspring. Initially, the parental chromosomes are packaged in two haploid nuclei, or pronuclei, each surrounded by a nuclear envelope (NE). For chromosome mixing to occur, the NE of the two pronuclei must somehow be breached or broken down. The NE is made of two membranes: an inner nuclear membrane and an outer nuclear membrane (Schooley *et al.*, 2012; Walters *et al.*, 2012). The outer nuclear membrane and the lumen between the two nuclear membranes are continuous with the endoplasmic reticulum (ER). Traversing these two membranes are nuclear pore complexes (NPCs), which allow selective transport of proteins and RNAs between the nucleus and cytoplasm. Underlying the inner nuclear membrane is the nuclear lamina, the main components of which are intermediate filaments composed of lamins (Burke and Stewart, 2013; Amendola and van Steensel, 2014). The nuclear lamina provides mechanical rigidity to the nucleus and, along with proteins associated with the inner nuclear membrane, contributes to chromatin-related processes, such as chromatin organization and transcription.

In interphase, chromosomes are confined to the nucleus and are separated from cytoplasmic centrosomes by the NE. Nuclear envelope breakdown (NEBD) begins in prophase/prometaphase, allowing microtubules emanating from centrosomes access to

This article was published online ahead of print in MBoC in Press (http://www.molbiolcell.org/cgi/doi/10.1091/mbc.E15-04-0244) on October 21, 2015.

M.M.R., M.M., K.K., S.S., T.M.-R., and O.C.-F. designed the experiments; M.M.R., M.M., K.K., B.L., and T.M.-R carried out the experiments; M.M.R. and O.C.-F. wrote the initial draft of the manuscript; and M.M.R., K.K., B.L., S.S., M.M., T.M.-R., and O.C.-F. edited the final version of the manuscript.

The authors declare that they have no conflict of interest.

Address correspondence to: Orna Cohen-Fix (ornac@helix.nih.gov).

Abbreviations used: ER, endoplasmic reticulum; NE, nuclear envelope; NEBD, nuclear envelope breakdown; NPC, nuclear pore complex.

chromosomes. During NEBD, the permeability barrier of the NE is breached as NPCs and the nuclear lamina disassemble and disperse (Güttinger *et al.*, 2009). NEBD is further aided by microtubules that bind to, and tear apart, the NE (Beaudouin *et al.*, 2002; Salina *et al.*, 2002). The process of NEBD is largely driven by the mitotic kinase Cdk1 (Heald and McKeon, 1990; Peter *et al.*, 1990; Dessev *et al.*, 1991), which phosphorylates many components of the NE, including subunits of the NPC, lamins and proteins associated with the inner nuclear membrane (Álvarez-Fernández and Malumbres, 2014). The VRK1 kinase also affects the NE by phosphorylating the barrier to autointegration (BAF) protein (Gorjánácz *et al.*, 2007; Molitor and Traktman, 2014). BAF binds both chromatin and inner nuclear membrane proteins containing a LEM domain. In the absence of VRK1 kinase activity, BAF fails to dissociate from the DNA, interfering with NE reassembly at the end of mitosis and likely also with NEBD (Gorjánácz *et al.*, 2007; Molitor and Traktman, 2014). Other mitotic kinases, such as Aurora A (Portier *et al.*, 2007; Hachet *et al.*, 2012) and polo-like kinase 1 (Plk1; see later discussion), have also been implicated in NEBD, but whether they affect the process directly or through the activation of processes upstream of NEBD is not known.

In *Caenorhabditis elegans* early embryos, changes in the permeability of the NE occur before the disassembly of the nuclear lamina; the permeability barrier of the NE is breached during prometaphase, resulting in spindle formation and chromosome movement within the perimeter of a NE with a seemingly intact nuclear lamina (Askjaer *et al.*, 2002; Gorjánácz *et al.*, 2007; Hachet *et al.*, 2007; Portier *et al.*, 2007; Hayashi *et al.*, 2012). A similar situation occurs in *Drosophila* early embryos (Paddy *et al.*, 1996; Katsani *et al.*, 2008), suggestive of a conserved process. NE permeabilization in *C. elegans* is likely facilitated by the dissociation of certain NPC components from the complex either throughout the NE (e.g., NPP-5 and MEL-28; Franz *et al.*, 2005; Galy *et al.*, 2006) or specifically at the NE that is adjacent to the centrosomes (e.g., NPP-3; Hachet *et al.*, 2012). This, and perhaps local NE openings, allows centrosome-anchored microtubules to contact chromosome through NE fenestrations of unknown nature. The nuclear lamina and the remaining NPC subunits disassemble only during metaphase/anaphase (Lee *et al.*, 2000), similar to *Drosophila* early embryos, but later than the timing of nuclear lamina disassembly in vertebrate cells, which occurs in prophase/prometaphase.

The breakdown of the NE after fertilization is not well characterized, especially in vertebrates, where visualizing this process is challenging. Broadly speaking, the association of the maternal and paternal pronuclei can happen in one of two ways (Szabo and O'Day, 1983): the NEs of the two pronuclei can fuse (as is the case for nuclei of gametes in a variety of fungi, algae, and higher plants) or, once the two pronuclei are in close apposition, their NEs can break down, leading to the mixing of their contents. The latter mechanism is common in vertebrates such as mouse (Zamboni *et al.*, 1972) and human (Zamboni *et al.*, 1966), although it has been suggested that pronuclear fusion can take place in in vitro–fertilized human oocytes (see, e.g., Levron *et al.*, 1995; van der Heijden *et al.*, 2009). In the fish *Oryzias* (Iwamatsu and Kobayashi, 2002) and in rabbit (Gondos *et al.*, 1972), nucleoplasmic bridges form between the two pronuclei before complete NE disassembly. These nucleoplasmic bridges necessitate the formation of pores that span four membranes—the two inner and two outer nuclear membranes of both pronuclei. When such pores form between nuclei that undergo fusion in single-cell organisms such as budding yeast (Melloy *et al.*, 2007), they do so by fusing the outer nuclear membranes of both nuclei, followed by fusing the two inner nuclear membranes. The mechanisms by which pronuclear nucleoplasmic bridges form in at least some vertebrates, and the extent to which they form after human fertilization, are not known.

In the present study, we examine the role of *C. elegans* PLK-1 in NEBD. PLK-1 is the nematode homologue of polo-like kinase (Plk1; also known as Polo in *Drosophila*, where it was first discovered, and Cdc5 in budding yeast), a conserved serine/threonine kinase involved in multiple aspects of mitosis, including centrosome maturation, spindle formation, chromosome condensation, kinetochore–microtubule attachments, sister chromatid separation, and cytokinesis (Petronczki *et al.*, 2008; Archambault and Glover, 2009). Complete absence of Plk1 activity results in the formation of a monopolar spindle in *Drosophila* (Sunkel and Glover, 1988), a prolonged prophase due to a delay in Cdk1 activation and a prometaphase arrest in both cultured animal cells (Lénárt and Peters, 2006) and in mouse one-cell embryos (Baran *et al.*, 2013), and inhibition of cytokinesis in budding yeast (Kitada *et al.*, 1993). Plk1 is also essential for the faithful execution of meiosis (Abrieu *et al.*, 1998; Tong *et al.*, 2002; Solc *et al.*, 2015). Plk1 phosphorylates a number of NE-associated proteins, including subunits of the NPC (Santamaria *et al.*, 2010; Grosstessner-Hain *et al.*, 2011; Hegemann *et al.*, 2011; Kettenbach *et al.*, 2011; Laurell *et al.*, 2011; Bibi *et al.*, 2013) and $p150^{Glued}$, a subunit of the dynein/dynacin complex (Li *et al.*, 2010) that participates in microtubule-dependent tearing of the NE during mitosis. Moreover, Plk1 is one of several kinases needed for efficient NPC disassembly (Laurell *et al.*, 2011). NE permeabilization still occurs when Plk1 is inactivated by chemical inhibition (Sumara *et al.*, 2004; Lénárt and Peters, 2006; Lénárt *et al.*, 2007; Petronczki *et al.*, 2007; Watanabe *et al.*, 2009), but in these studies, the integrity of the nuclear lamina was not examined directly. Thus a role of PLK1 in the timely disassembly of the nuclear lamina remains to be explored.

In *C. elegans*, RNA interference (RNAi) treatment against PLK-1 caused oocytes to delay in prophase of meiosis I with aberrantly retained NE, which eventually broke down after fertilization (Chase *et al.*, 2000). The authors of that study concluded that PLK-1 is needed for NEBD in the oocyte, but given the multitude of processes that require PLK-1, it is conceivable that inhibition of PLK-1 led to a cell cycle delay well before NEBD itself. Moreover, because of the meiotic arrest, NEBD outside meiosis could not be examined.

Here we show that in *C. elegans*, PLK-1 is required for complete NEBD during early embryogenesis and that this function of PLK-1 is essential for mixing the maternal and paternal genomes after fertilization. When PLK-1 was partially inactivated, mitosis progressed in a timely manner, but chromosomes failed to align properly at metaphase, and the NE remained intact. Our data further suggest that proper chromosome alignment is needed for the breakdown of the NE between the maternal and paternal pronuclei.

RESULTS

Partial inactivation of PLK-1 results in the formation of paired nuclei in each cell of early *C. elegans* embryos

In *C. elegans*, after fertilization, the maternal and paternal pronuclei migrate toward each other and come into very close proximity, as evident by the flattening of the two pronuclei at the interface of interaction (Gönczy *et al.*, 1999; Poteryaev *et al.*, 2005). At this stage, the one-cell embryo undergoes its first mitosis, and a single nucleus is formed in each of the two daughter cells. The Bowerman lab previously isolated a temperature-sensitive *plk-1* allele, *plk-1(or683ts)* (henceforth $plk\text{-}1^{ts}$), which after the first mitosis produces two nuclei in each daughter cell (O'Rourke *et al.*, 2011). The *or683ts* mutation in *plk-1* results in a methionine-to-lysine substitution in amino acid

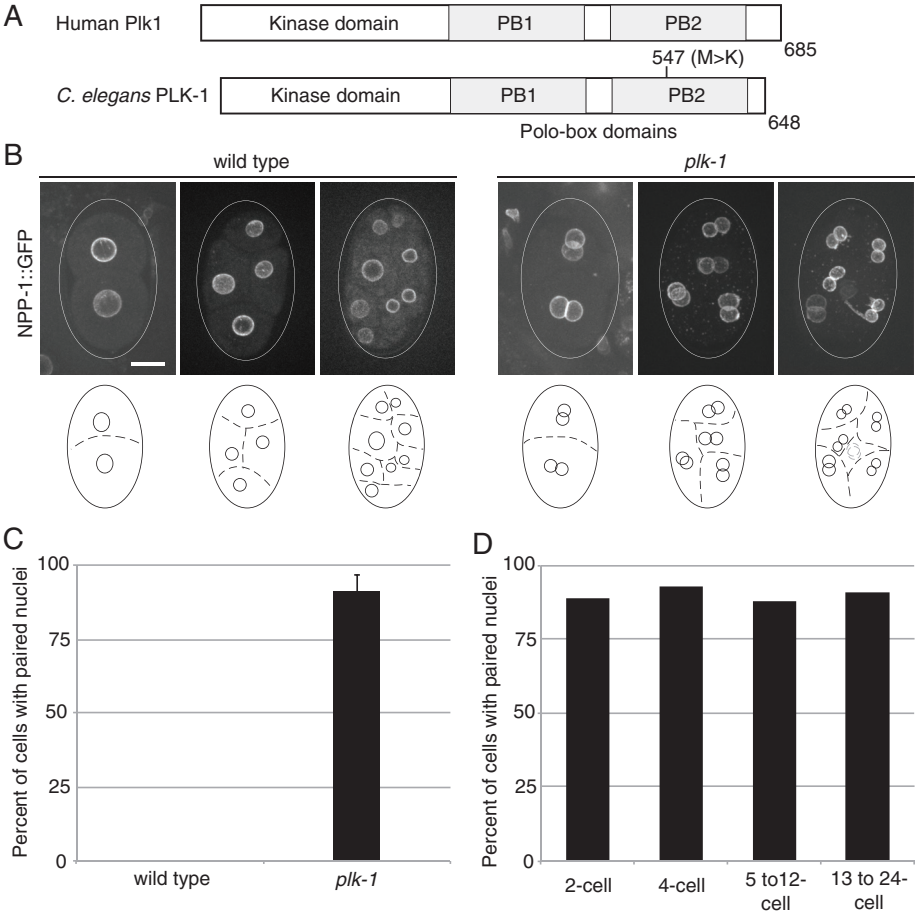

FIGURE 1: Partial down-regulation of the PLK-1 protein results in the formation of paired nuclei in each cell of *C. elegans* early embryos. (A) Schematic diagram of human Plk1 and *C. elegans* PLK-1 functional domains. The *plk-1(or683ts)* allele carries a mutation that causes a methionine-to-lysine change in amino acid 547. (B) Examples of two-cell, four-cell, and multicell embryos of wild-type (left) and *plk-1*^{ts} (right) strains grown at 23°C. The NE was visualized with an NPC subunit, NPP-1, fused to GFP (NPP-1::GFP). Bar, 10 µm. (C) Quantification of the paired-nuclei phenotype. For each strain (wild type, $n = 625$; *plk-1*^{ts}, $n = 1080$), the percentage of cells with paired nuclei was calculated out of the total number of cells in all embryos examined. No cells with paired nuclei were observed in wild-type embryos. Error bars indicate SD. (D) Quantification of the paired-nuclei phenotype in *plk-1*^{ts} embryos from C, displayed by embryonic stage. The number of cells scored was 102, 176, 488, and 257 for embryos with two, four, 5–12, and 13–24 cells, respectively. The fraction of cells with paired nuclei did not change during the first few embryonic divisions.

547 within the second polo-box domain (Figure 1A). In our hands, *plk-1*^{ts} animals shifted to the nonpermissive temperature (26°C) at the L1 stage were sterile (100%, $n = 62$). At a semipermissive temperature (23°C), however, *plk-1*^{ts} embryos exhibited a highly penetrant "paired-nuclei" phenotype that persisted through several divisions (Figure 1, B–D; here and in all subsequent figures, images of embryos are shown with the anterior end at the bottom, whereas images of nuclei/chromosomes are shown with the anterior end to the left). Paired nuclei could also be seen after RNAi treatment against PLK-1 in wild-type animals, albeit to a lesser extent (14% of embryos [$n = 95$] exhibited at least one cell with paired nuclei; Supplemental Figure S1A). Varying degrees of this RNAi-induced phenotype were observed previously, although not examined further (Nishi *et al.*, 2008; Rivers *et al.*, 2008; Noatynska *et al.*, 2010). These results suggest that *plk-1*^{ts} is not a specialized allele but instead causes a partial loss of PLK-1 function at the semipermissive temperature. PLK-1 is known to be required for meiosis (Chase *et al.*, 2000), but at the semipermissive temperature, the two meiotic divisions in *plk-1*^{ts} animals were probably executed successfully, because 100% of embryos had two polar bodies ($n = 64$), although the brood size was smaller (Supplemental Figure S1B). *plk-1*^{ts} embryos grown at the semipermissive temperature eventually died (Supplemental Figure S1C). Whether this was due to the persistence of paired nuclei or a defect in another PLK-1–dependent process is not known.

The paired nuclei are attached to each other by a mechanism other than membrane fusion

Curiously, the paired nuclei in cells of *plk-1*^{ts} embryos always remained in contact with each other throughout interphase (Figure 1B), suggesting that they are somehow linked. To examine the nature of the interface between the paired nuclei, we examined interphase cells from four-cell embryos by electron microscopy (Figure 2 and Supplemental Figure S2). The NEs of the two nuclei did not appear to be fused ($n = 16$). Instead, all paired nuclei examined displayed an extended gap between the flattened membranes of the juxtaposed nuclei. Serial sectioning of paired nuclei at 70-nm sections showed that the nuclei maintain a constant distance at the flattened region (Figure 2). The internuclear gap often contained cytoplasmic material, such as membranes, microtubules, and ribosomes (Supplemental Figure S2). We did not detect any structures connecting the two nuclei, suggesting that if such structures exist, their size is below the limit of detection.

PLK-1 is required for complete NPC dissociation from the NE after pronuclear meeting

To determine the source of the paired nuclei, we followed wild-type and *plk-1*^{ts} embryos by live-cell imaging from fertilization to the four-cell stage at 23°C, using the NPC subunit NPP-1 fused to green fluorescent protein (NPP-1::GFP) as a marker for the NE. In wild-type one-cell embryos, the two pronuclei met, and the cell then entered mitosis, as evident by chromosome congression (Figure 3A and Supplemental Movie S1). NPCs began to dissociate from the NE in metaphase and were completely disassembled by anaphase (Figure 3, A, C, D, and F, and Supplemental Movie S1), as reported previously (Lee *et al.*, 2000). The NPCs reassembled around the segregated chromosomes at late anaphase/telophase, forming a single nucleus in each cell (Figure 3A and Supplemental Movie S1). In *plk-1*^{ts} embryos, the pronuclei met and chromosome congression commenced as in the wild type (Figure 3B and Supplemental Movie S2). However, unlike in wild-type embryos, in *plk-1*^{ts} one-cell embryos, NPP-1 persisted at the NE throughout metaphase and, in most embryos, throughout anaphase (Figure 3, B, C, E, and G, and Supplemental Movie S2). Thus down-regulation of PLK-1 disrupts at least some aspects of NEBD.

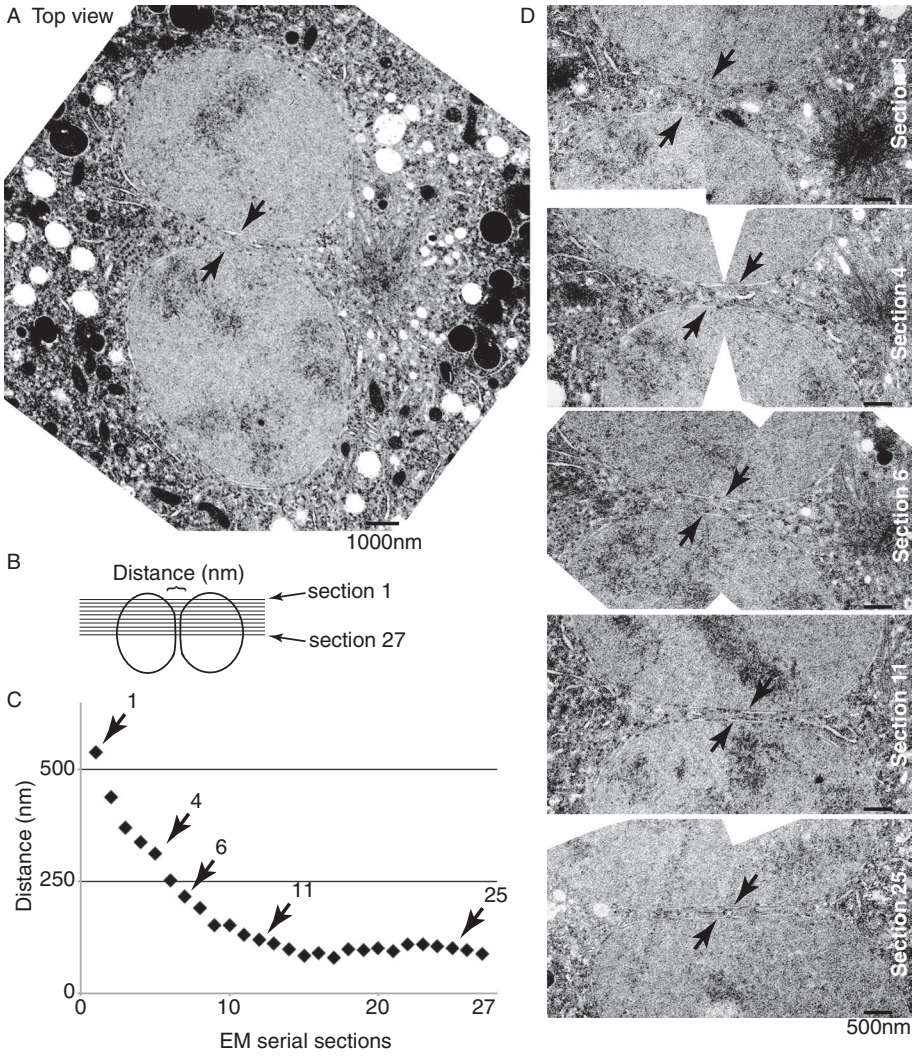

FIGURE 2: In *plk-1*^{ts} embryos, paired nuclei in interphase are not fused. (A) Electron micrograph of paired nuclei in interphase from a four-cell *plk-1*^{ts} embryo grown at 23°C. Bar, 1000 nm. (B) Cartoon depicting the positions of serial sections that were used to measure the distance between the paired nuclei shown in A. (C) Graph showing the distances (in nanometers) between two nuclear membranes in 27 sequential electron micrograph sections of the paired nuclei shown in A. The distance between each section is 70 nm. Arrows point to sections shown in D. (D) Enlargements of selected sections from C. Bar, 500 nm. Black arrows in A and D point to the nuclear membranes of each nucleus of the paired nuclei. For additional examples of electron micrographs of paired nuclei, see Supplemental Figure S2.

Another phenotype that was apparent in *plk-1*^{ts} one-cell embryos grown at the semipermissive temperature was a defect in chromosome congression to the metaphase plate (henceforth termed chromosome congression) and the alignment of the maternal and paternal metaphase plates relative to each other (henceforth termed metaphase plate alignment). This was determined based on chromosome configuration immediately before anaphase using time-lapse microscopy. In wild-type one-cell embryos, immediately before anaphase, all chromosomes had congressed to the metaphase plate, and the metaphase plates of the maternal and paternal pronuclei were always aligned with each other (Figure 3H, top). In contrast, in 81.2% of *plk-1*^{ts} one-cell embryos, the chromosomes failed to completely congress and/or the metaphase plates failed to align ($n = 32$; Figure 3H, bottom). As will be discussed later, this defect in chromosome congression and metaphase plate alignment may be a contributing factor in the formation of paired nuclei in daughter cells.

The persistence of NPP-1::GFP around mitotic chromosomes of *plk-1*^{ts} embryos was also seen in subsequent cell divisions (Figure 4). The daughter cells that arise from division of the one-cell embryo are designated AB (at the anterior end) and P1 (at the posterior end). The division of the two-cell embryo is asynchronous, with the AB cell dividing before the P1 cell (Gönczy and Rose, 2005; Rose and Gönczy, 2014). In wild-type AB and P1 cells, NPP-1::GFP was present in most metaphases but was completely absent during anaphase (Figure 4, A, C, and D, and Supplemental Movie S3). In contrast, in most *plk-1*^{ts} embryos, the NE association of NPP-1::GFP persisted through metaphase and anaphase of both AB and P1 cells (Figure 4, B–D, and Supplemental Movie S4), and each cell in four-cell embryos contained paired nuclei (Figure 4B and Supplemental Movie S4). Thus down-regulation of PLK-1 leads to a persistent defect in NPP-1 dissociation from the NE during mitosis throughout early embryogenesis.

PLK-1 is required for mixing of maternal and paternal chromosomes

A paired-nuclei phenotype was previously reported for down-regulation of the RAB-5 GTPase, the ER-shaping proteins YOP-1 and RET-1, the NPC component NPP-12/gp210, and the phosphatidic acid hydrolase LPIN-1 (Audhya *et al.*, 2007; Galy *et al.*, 2008; Golden *et al.*, 2009; Gorjanacz and Mattaj, 2009). In these studies, live-cell imaging suggested that this phenotype was due to a defect in NEBD, resulting in a failure in mixing maternal and paternal chromosomes, which consequently remained in different nuclei. Consistent with this also being the case for the paired nuclei of *plk-1*^{ts} embryos, we observed that whereas in wild-type one-cell embryos, the maternal and paternal chromosomes form a continuous line in metaphase and anaphase ($n = 30$), in most *plk-1*^{ts} one-cell embryos ($n = 22$ of 26), there was a gap between the maternal and paternal chromosomes during both metaphase and anaphase (Figure 5 and Supplemental Figure S3).

To examine further whether the maternal and paternal chromosomes truly remain separated in the *plk-1*^{ts} embryo, we used a genetic scheme to distinguish between maternally and paternally derived chromosomes based on the presence or absence of trimethylation of Lys-27 on histone H3 (H3K27me3). H3K27me3 is generated by polycomb repressive complex 2 (PRC2), which in *C. elegans* is composed of three subunits, MES-2, MES-3, and MES-6 (Capowski *et al.*, 1991). Parent worms lacking MES-3 generate gametes whose chromosomes lack H3K27me3 (Bender *et al.*, 2004; Gaydos *et al.*, 2014). Of note, embryos that inherit one set of chromosomes from a wild-type parent and another set from a parent lacking PRC2 maintain differentially marked chromosomes through many cell divisions (Gaydos *et al.*, 2014; Figure 6A; note the presence of

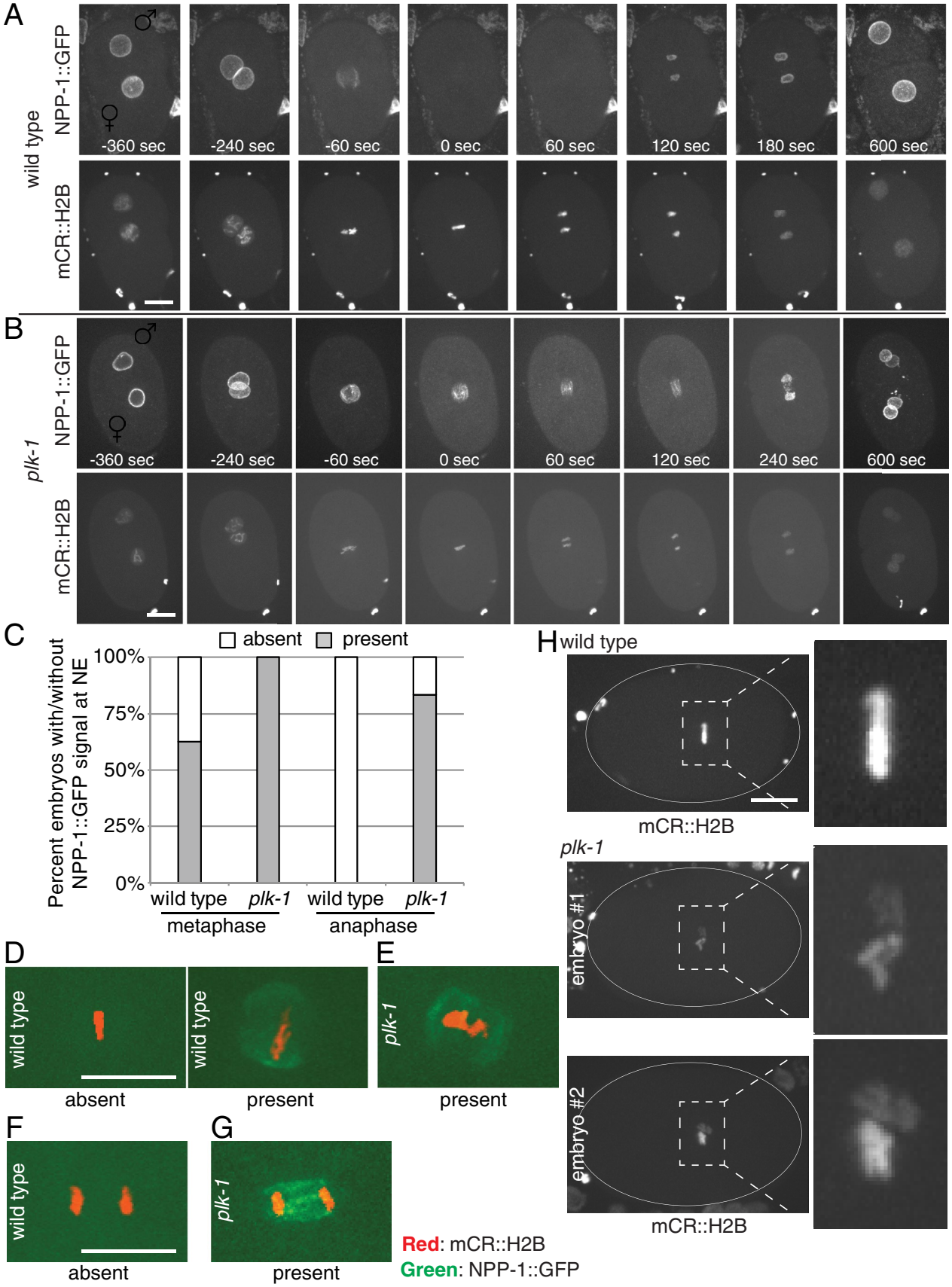

FIGURE 3: *plk-1*^{ts} embryos exhibit incomplete NPC dissociation and abnormal chromosome congression during mitosis. (A, B) Time-lapse sequence of wild-type (A) and *plk-1*^{ts} (B) embryos expressing NPP-1::GFP as they undergo the first mitotic division. Time 0 is defined as the metaphase time point. In the wild-type embryo, the NPP-1::GFP signal is absent

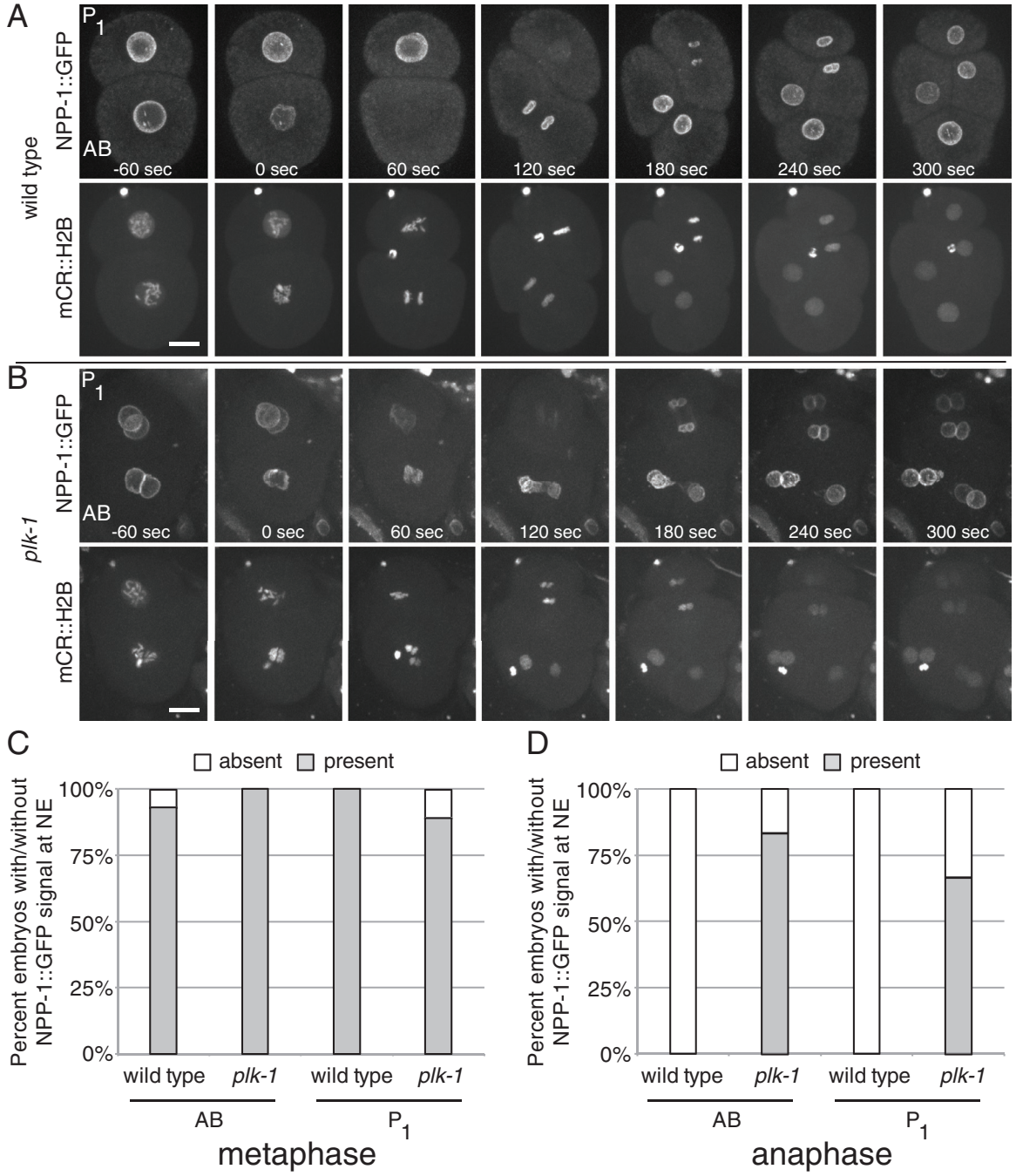

FIGURE 4: NPC disassembly defect persists in *plk-1*^{ts} embryos during the second round of mitosis. (A, B) Time-lapse images of wild-type (A) and *plk-1*^{ts} (B) embryos expressing NPP-1::GFP and mCherry::H2B as they undergo the second round of cell division in the AB (lower cell) and P1 (upper cell) cells. Time 0 was defined as metaphase of the AB cell (the first cell to divide). Bar, 10 µm. (C, D) Quantification of the NPP-1::GFP pattern during metaphase (C) and anaphase (D) of AB and P1 cells, based on time-lapse images such as the one shown in A and B (nine time lapses for both wild type and *plk-1*^{ts}).

in both metaphase and anaphase (t = 0 and 60 s), whereas in the *plk-1*^{ts} embryo, NPP-1::GFP is present throughout mitosis. DNA is labeled by histone H2B tagged with mCherry (mCR::H2B). Male and female symbols mark the paternal and maternal pronuclei, respectively. Bar, 10 µm. (C) Quantification of the NPC disassembly defect, as assayed by NPP-1::GFP dissociation, during the first mitotic division based on time-lapse movies as shown in A and B. Number of time-lapse movies analyzed was nine and 17 for wild type and *plk-1*^{ts}, respectively. (D, E) Examples of the NPP-1::GFP pattern during metaphase in wild-type (D) and *plk-1*^{ts} (E) embryos. DNA was visualized using mCherry::H2B. Bar, 10 µm. (F, G) Examples of the NPP-1::GFP pattern during anaphase in wild-type (F) and *plk-1*^{ts} (G) embryos. DNA was visualized using mCherry::H2B. Bar, 10 µm. (H) Chromosome configuration during metaphase in wild type (top) and *plk-1*^{ts} (middle and bottom) in one-cell embryos. Typical chromosome congression and alignment defects observed in most *plk-1*^{ts} embryos during the first mitosis. Of 32 one-cell embryos examined, 81.25% had either or both defects. Bar, 10 µm.

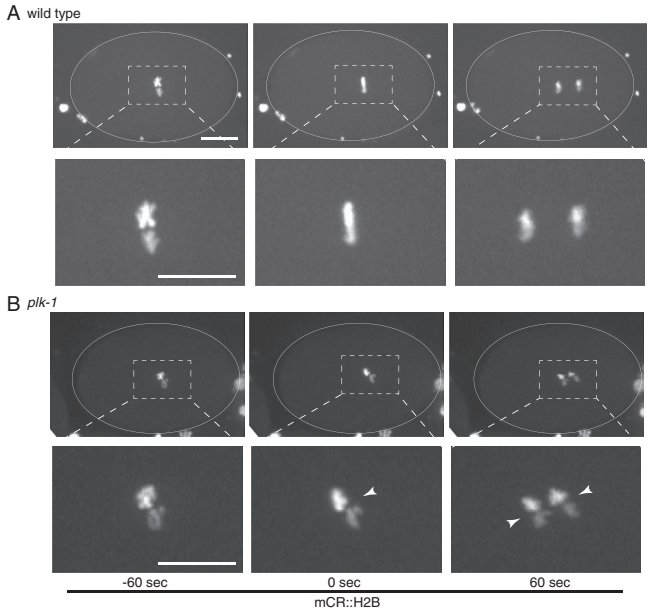

FIGURE 5: PLK-1 down-regulation leads to a persistent gap between maternal and paternal chromosomes. (A) A wild-type embryo going through the first mitotic division after fertilization. At metaphase ($t = 0$), maternal and paternal DNA form a continuous line before separation of chromosomes in anaphase ($t = 60$ s). DNA was visualized using mCherry::H2B. Bar, 10 μm. (B) A *plk-1*^{ts} embryo going through the first mitotic division after fertilization. A gap (arrowhead) between two DNA masses persists through metaphase ($t = 0$ s) and anaphase ($t = 60$ s). DNA was visualized using mCherry::H2B. See additional examples in Supplemental Figure S3. Bar, 10 μm.

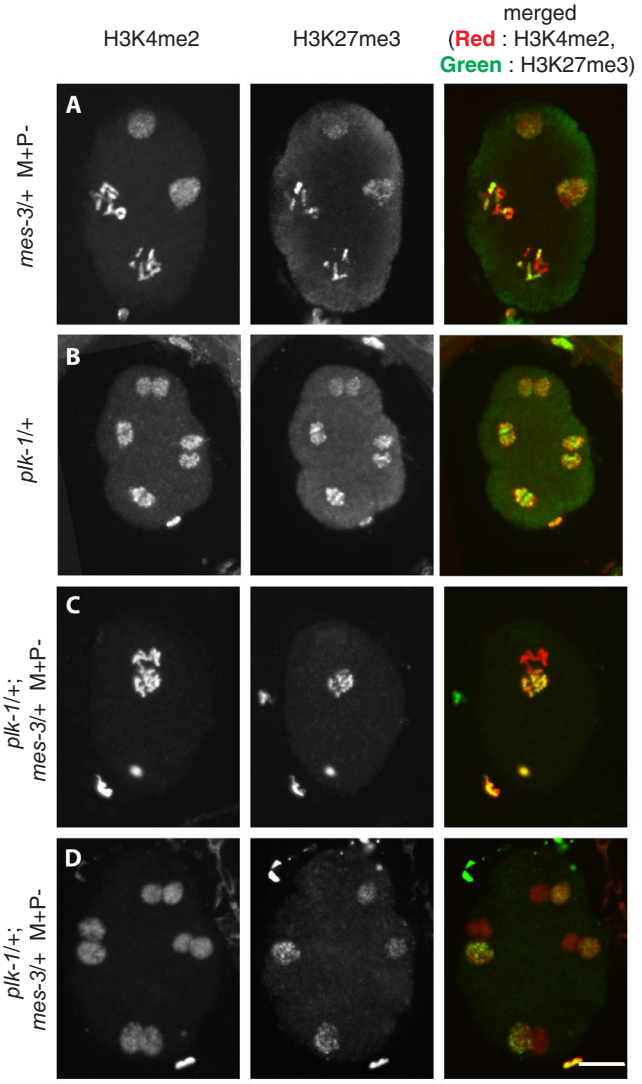

FIGURE 6: Maternally and paternally derived chromosomes remain in separate nuclei in cells of *plk-1*^{ts} embryos. In all cases, embryos were produced by mating feminized hermaphrodites (which produce no sperm; *fem-2* in A and *fog-1* in all other panels) with male worms. M+P– denotes that the maternal chromosomes were from a mother that was wild type for *mes-3* (M+), whereas the paternal chromosomes were from a *mes-3* mutant male (P–). (A) Images of a *mes-3/+* M+P– four-cell embryo. In each nucleus, H3K4me2 (red) is on all chromosomes, whereas H3K27me3 (green) is only on maternal chromosomes. (B) Images of a *plk-1*^{ts}*/+* four-cell embryo, generated by mating a *fog-1; plk-1* hermaphrodite with a wild-type male. Each cell contains a pair of nuclei with both H3K4me2 and H3K27me3 on all chromosomes. (C, D) Images of *plk-1*^{ts}*/+; mes-3/+* M+P– embryos, generated by mating *fog-1; plk-1*^{ts} mutant feminized hermaphrodites with *mes-3* mutant males. In the one-cell embryo (C), H3K4me2 is on maternal and paternal chromosomes, whereas H3K27me3 is only on maternal chromosomes. In the four-cell embryo (D), each cell contains a pair of nuclei, both with H3K4me2. Only one nucleus in each cell has maternally contributed H3K27me3. Bar, 10 μm.

H3K4me2 marked chromosomes [red] that are not marked by H3K27me3 [green]). After mating of *plk-1*^{ts} females with wild-type males, the embryos displayed a paired-nuclei phenotype due to partial inactivation of maternally supplied PLK-1 (from the *plk-1*^{ts} allele) and lack of zygotic expression from the male-contributed *plk-1* gene at this early embryonic stage (Figure 6B). After mating *plk-1*^{ts} females with *mes-3* mutant males, maternally and paternally derived chromosomes were differentially marked: maternal (M+) chromosomes had H3K27me3, whereas paternal (P–) chromosomes lacked H3K27me3 (Figure 6C). Of importance, after cell division, 93% of cells ($n = 91$) in these embryos exhibited paired nuclei, and in 100% of those cells, the H3K27me3+ maternal chromosomes were in one nucleus and the H3K27me3– paternal chromosomes were in the other nucleus (Figure 6D). This finding demonstrates that the paired nuclei in *plk-1*^{ts} embryos maintain separation of maternal and paternal chromosomes and supports the notion that PLK-1 is required for the intermingling of maternal and paternal chromosomes.

PLK-1 is needed for the breakdown of the NE between the maternal and paternal nuclei

The failure in maternal and paternal chromosome mixing in *plk-1*^{ts} pointed to a general defect in NEBD. To examine this further, we followed two additional NE proteins, LMN-1 and LEM-2, through the first two embryonic cell divisions. LMN-1 is the single *C. elegans* lamin homologue, homologous to lamin B, and LEM-2 is an integral nuclear membrane protein homologous to the human LEMD2 protein (Lee *et al.*, 2000; Brachner *et al.*, 2005). As shown previously (Lee *et al.*, 2000), in one-cell wild-type embryos, LMN-1::yellow fluorescent protein (YFP) persists around the chromosomes until metaphase and is usually absent in anaphase (Figure 7, A and E, and Supplemental Movie S5). In contrast, in *plk-1*^{ts} embryos, LMN-1::YFP was visible in the vast majority of one-cell anaphases and in particular between the maternal and paternal chromosomes (Figure 7, B–E, and Supplemental Movie S6). Because LMN-1 is homologous to lamin B and as such is predicted to be associated with the NE, this

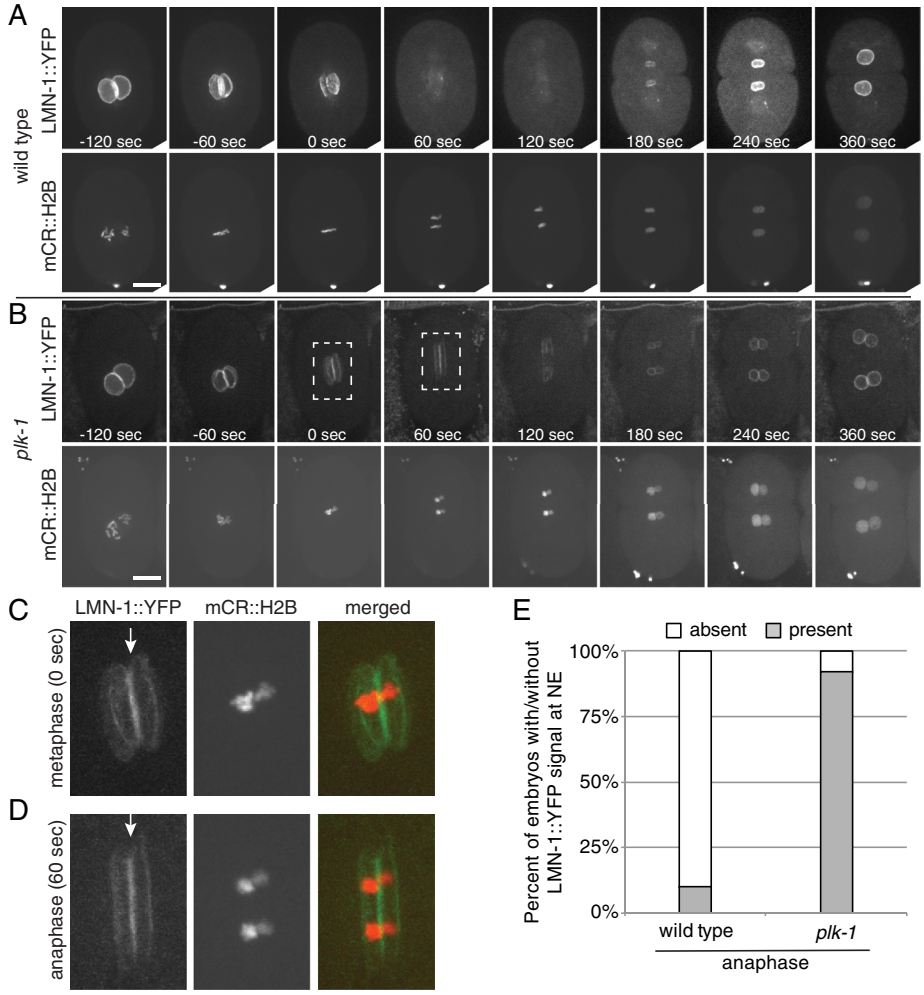

FIGURE 7: PLK-1 is needed for proper nuclear lamin disassembly in one-cell embryos. (A) Time-lapse images of a wild-type embryo expressing LMN-1::YFP and mCherry::H2B undergoing the first mitotic division after fertilization. Metaphase was denoted as time 0. Note that LMN-1::YFP is not detectable during anaphase (t = 120 s). Bar, 10 µm. (B–D) Time-lapse images of a *plk-1*^{ts} embryo, as in A. LMN-1::YFP is visible during both metaphase (t = 0 s) and anaphase (t = 60 s) and in particular between the maternal and paternal chromosomes. Here C and D are enlargements of the boxed areas in metaphase and anaphase, respectively, of B. Bar, 10 µm. (E) Quantification of LMN-1::YFP signal during anaphase, based on time-lapse images as in A and B. Here n = 10 and 12 for wild type and *plk-1*^{ts}, respectively.

observation suggests that in *plk-1*^{ts} one-cell embryos, the NE between the maternal and paternal pronuclei fails to disassemble.

The presence of LMN-1::YFP around anaphase chromosomes was also seen during mitosis in two-cell *plk-1*^{ts} embryos (in the AB and P1 cells; Figure 8, B and C, and Supplemental Movie S7). Thus the NE between the maternal and paternal chromosomes is present even after the one-cell stage, explaining how the paired-nuclei phenotype persists throughout early embryogenesis. Of interest, in wild-type embryos, LMN-1::YFP dissociated from the NE in anaphase of the AB cells but was present in ~ 80% of P1 cell anaphases (Figure 8, A and C). However, because the NE dissociates completely in one-cell wild-type embryos, the persistence of LMN-1::YFP, and hence the NE, at the periphery of wild-type P1 mitotic chromosomes does not result in the formation of paired nuclei.

During early embryogenesis, PLK-1 is diffusely distributed throughout the entire cell in interphase and is associated with chromosomes during mitosis (Chase *et al.*, 2000; Budirahardja and Gönczy, 2008; Nishi *et al.*, 2008). Of importance, in the two-cell embryo, PLK-1 is present in a gradient, with a higher concentration in the cytoplasm of the AB cell than in the P1 cell (Chase *et al.*, 2000; Budirahardja and Gönczy, 2008; Nishi *et al.*, 2008). If this gradient of PLK-1 were responsible for the different degrees of LMN-1 dissociation from the NE during anaphase of the AB versus the P1 cell, then abolishing this gradient should equalize the two cells. The PLK-1 gradient is established and maintained by PAR proteins (Nishi *et al.*, 2008; Rivers *et al.*, 2008). Therefore, to abolish the PLK-1 gradient, wild-type animals expressing LMN-1::YFP were treated with RNAi against PAR-1, PAR-2, and PAR-5, simultaneously. The PLK-1 gradient contributes to the asynchrony in cell division between the AB and P1 cells (Budirahardja and Gönczy, 2008). The effectiveness of the RNAi treatment in redistributing PLK-1 was evident by the simultaneous divisions of the AB and P1 cells (Figure 8D). In all cases, when the PLK-1 gradient was disrupted, LMN-1::YFP was no longer visible during anaphase of the P1 cell (n = 12). Although we cannot exclude the possibility that an asymmetrically distributed protein other than PLK-1 is responsible for the incomplete dissociation of LMN-1::YFP from the NE in wild-type P1 cells, our data are consistent with a role for PLK-1 in LMN-1 dissociation from the NE during anaphase in wild-type cells.

We also examined the presence of LEM-2::GFP at the NE during early embryonic divisions. As shown previously (Lee *et al.*, 2000), in wild-type one-cell embryos, LEM-2::GFP initially surrounds both pronuclei and then persists throughout mitosis at the edge of the region occupied by the spindle (Figure 9A). LEM-2 is also visible in a membranous structure around centrosomes (Poteryaev *et al.*, 2005; Figure 9A). In one-cell *plk-1*^{ts} embryos, LEM-2::GFP persisted not only at the periphery of the chromatin region, but also between the maternal and paternal chromosomes (Figure 9B, n = 18). Because LEM-2 is a nuclear membrane protein, this observation is further evidence that in *plk-1*^{ts} embryos, the NE between the maternal and paternal chromosomes fails to disassemble. The persistence of LEM-2::GFP between the DNA masses that originated from the maternal and paternal pronuclei was also seen in the divisions of the AB and P1 cells (Figure 9C and Supplemental Movie S7; n = 9), explaining why the paired-nuclei phenotype persists throughout early embryonic divisions. Of interest, the analysis of LEM-2::GFP distribution in *plk-1*^{ts} embryos revealed that PLK-1 is also required for the formation of the ring-like structure around centrosomes (Figure 9, B and C; see later discussion).

The persistence of paired nuclei through multiple divisions of *plk-1*^{ts} embryos could be due to a requirement for PLK-1 in NEBD throughout early embryogenesis. Alternatively, PLK-1 may only be required during the first mitosis, and its absence creates a structure that the embryo has no way of resolving at later cell divisions. Because *plk-1*^{ts} is a temperature-sensitive mutant, we examined the

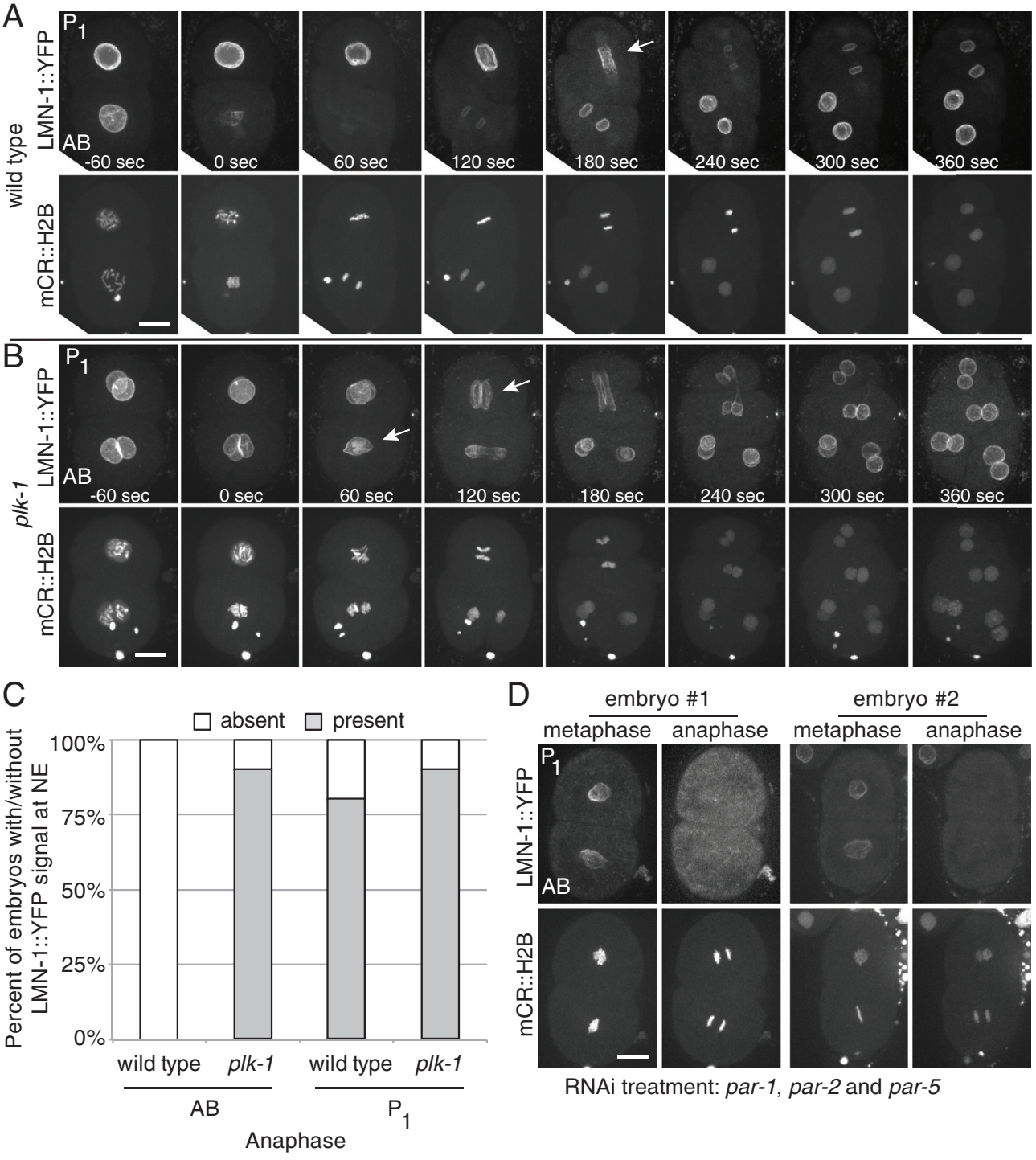

FIGURE 8: PLK-1 is required for complete nuclear lamin disassembly in wild-type two-cell embryos. (A, B) Time-lapse images of wild-type (A) and *plk-1*^{ts} (B) two-cell embryos expressing LMN-1::YFP and mCherry::H2B as they undergo the second round of mitosis in AB (lower cell) and P1 (upper cell). Time 0 was defined as the metaphase of the AB cell (the first cell to divide). In the wild-type embryo, LMN-1::YFP is undetectable during anaphase of the AB cell but is present during anaphase of the P1 cell (t = 180 s, arrow; see also C). In the *plk-1*^{ts} embryo, LMN-1::YFP is detectable during anaphase of both cells (t = 60 and 120 s, arrows). Bar, 10 μm. (C) Quantification of the presence/absence of LMN-1::YFP during anaphase of the AB and P1 cells in wild-type and *plk-1*^{ts} embryos, based on time-lapse images as shown in A and B. Here n = 10 for both wild type and *plk-1*^{ts}. (D) Metaphase and anaphase in two wild-type two-cell embryos expressing LMN-1::YFP and mCherry::H2B after *par* RNAi treatment. The effectiveness of the RNAi treatment is evident by the synchronous mitoses of the AB and P1 cells (compare to the lag between the two mitoses in A). LMN-1::YFP signal disappears completely from both AB and P1 cells. Bar, 10 μm.

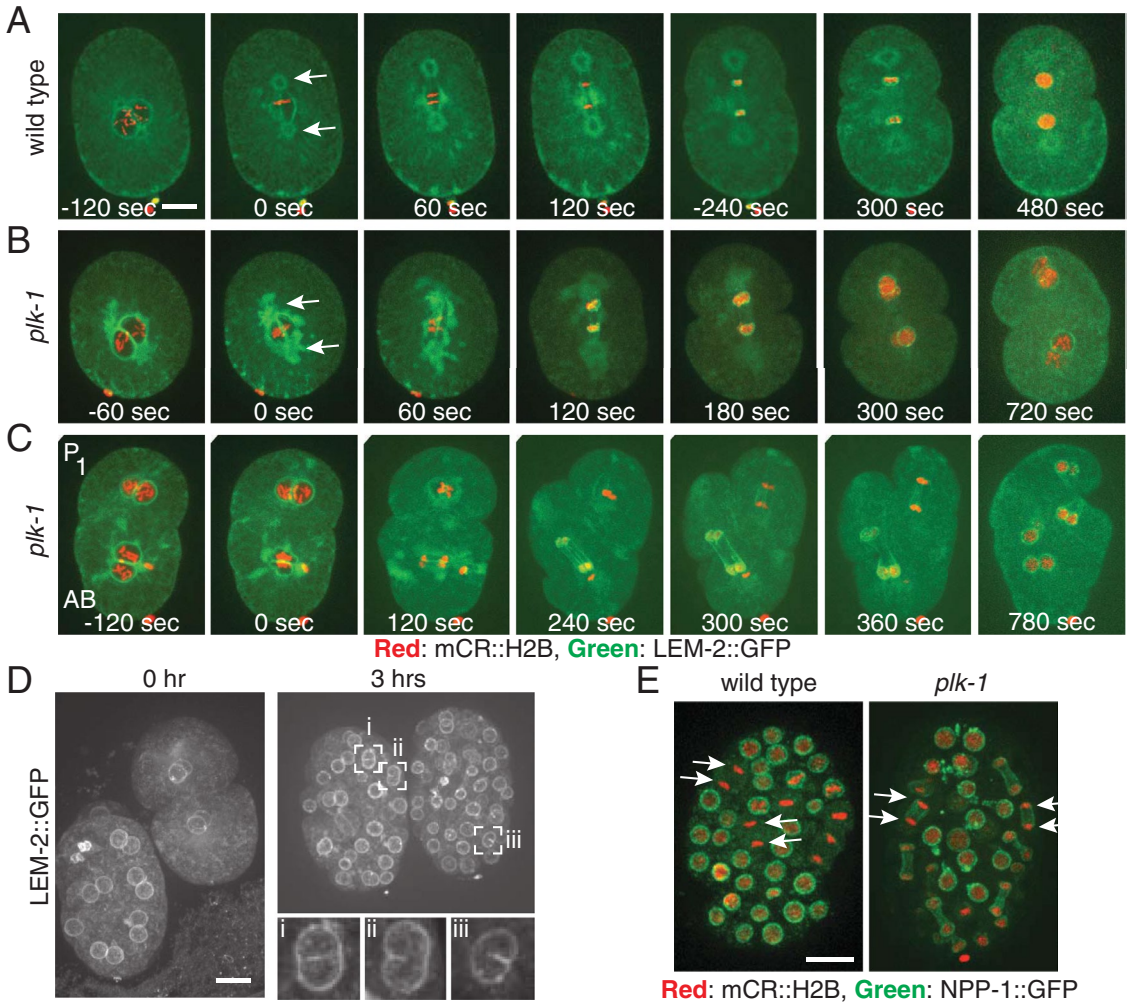

FIGURE 9: PLK-1 is involved in disassembly of the NE separating maternal and paternal DNA after fertilization and in later embryonic divisions. (A, B) Time-lapse images of a wild-type (A) and a *plk-1*^{ts} (B) embryo expressing LEM-2::GFP and mCherry::H2B undergoing the first mitosis. Note that LEM-2::GFP marking the NE between the maternal and paternal chromosomes disassembles in anaphase in the wild-type embryo (A, $t = 60$ s) but not in anaphase in the *plk-1*^{ts} embryo (B, $t = 60$ s). In addition, LEM-2::GFP appears in ring-like structures around centrosomes in the wild-type embryo, whereas the LEM-2::GFP structures in the *plk-1*^{ts} embryo are disorganized (see more on these structures later). Arrows point to ring-like structures (A) or disorganized structures (B) around centrosomes. (C) A *plk-1*^{ts} embryo expressing LEM-2::GFP and mCherry::H2B undergoing the second round of mitosis in AB (lower cell) and P1 (upper cell). A defect in NE disassembly persists through both mitoses (see time points 120–300 s in the AB cell), generating paired nuclei in all four daughter cells (780 s). Bar, 10 µm (A–C). (D) *plk-1*^{ts} embryos expressing LEM-2::GFP were collected from animals grown at 23°C (the semipermissive temperature) and then down-shifted to 16°C (the permissive temperature). Embryos were examined before the temperature down-shift (time = 0 h) and 3 h after the shift. Temperature-down-shifted *plk-1*^{ts} embryos exhibited a reduction in the fraction of cells with paired nuclei. Enlarged cells (i–iii) show examples of partial disassembly of the membrane between the two nuclei. Bar, 10 µm. (E) Wild-type and *plk-1*^{ts} embryos expressing NPP-1::GFP were collected from animals grown at 16°C and then up-shifted to 23°C. Embryos were examined before the temperature up-shift (see images in Supplemental Figure S4) and 2.5 h after the shift. Anaphase chromosomes in wild-type embryos were devoid of associated NE, whereas anaphase chromosomes in *plk-1*^{ts} embryos were surrounded by NE (arrows). NE can also be seen between the segregating chromosomes. NE appendages are associated with some interphase nuclei in *plk1*^{ts} embryos only. Bar, 10 µm.

fate of embryos with paired nuclei that were generated at the semi-permissive temperature but then were shifted down to the permissive temperature. After the temperature down-shift, the fraction of cells exhibiting paired nuclei was significantly reduced (from 87 ± 8.45% at time 0 [$n = 35$] to 28 ± 5.85% after 3 h at 16°C [$n = 68$]), and it was possible to detect nuclei in which the membrane between the two nuclei was only partially present (Figure 9D), as if PLK-1 reactivation promoted the disassembly of this part of the NE. Thus PLK-1 can promote NEBD beyond the one-cell stage.

To examine further the possible involvement of PLK-1 in NEBD beyond the first embryonic division, we carried out a reciprocal temperature up-shift experiment: early embryos (two- to eight-cell stage) from wild-type or *plk-1*^{ts} worms grown at the permissive temperature were imaged, up-shifted to 23°C for 2.5 h, and then reimaged. Before the temperature up-shift, all embryos had normal nuclei (namely, a single nucleus per cell; Supplemental Figure S4). After the temperature up-shift, in wild-type embryos, the NE disassembled before anaphase, such that in all anaphase cells ($n = 114$),

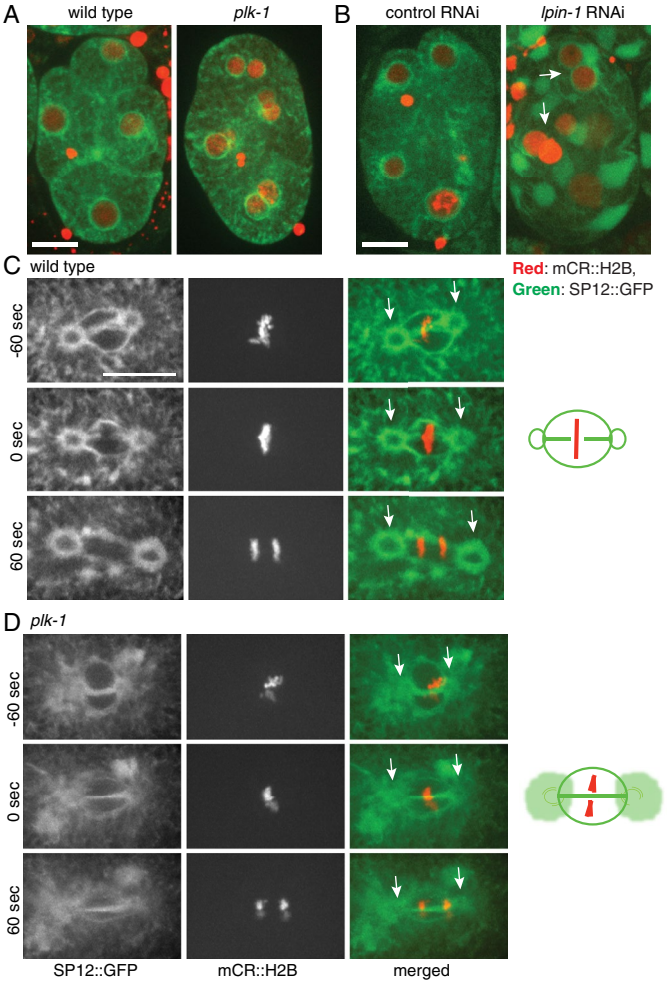

FIGURE 10: PLK-1 affects the organization of a membranous structure(s) around centrosomes but not peripheral ER structure. (A) Wild-type and *plk-1*^{ts} four-cell embryos expressing the ER marker SP12::GFP. (B) Six-cell embryos from control and *lpin-1* RNAi–treated animals expressing SP12::GFP. Note the paired nuclei in the *lpin-1* RNAi–treated embryos (arrows) indicative of LPIN-1 down-regulation. For more examples, see Supplemental Figure S5. (C, D) Time-lapse images of mitotic chromosomes in a wild-type (C) and a *plk-1*^{ts} (D) embryo expressing SP12::GFP and mCherry::H2B. Metaphase was denoted as time 0. Note the gap in the NEs near the metaphase chromosomes and the clear, thick rings at the poles in the wild-type embryo. Both are missing in the *plk-1*^{ts} embryo (arrows; see also Figure 9, A and B). Bar, 10 μm.

the chromosomes were devoid of any associated NE, as visualized by NPP-1::GFP (Figure 9E). In contrast, in 100% of anaphase cells of *plk-1*^{ts} embryos (n = 105), chromosomes were associated with NE, and NE was also present between the two segregating DNA masses (Figure 9E and Supplemental Figure S4). Some interphase nuclei were associated with clumps of NPP-1:::GFP, possibly representing NE that failed to disassemble in the preceding mitosis. Taken together, these observations suggest that PLK-1 is needed for complete NEBD not only during the first embryonic mitosis, but also during later embryonic cell divisions.

PLK-1 affects the organization of a membranous structure around the centrosomes but not general ER structure

As mentioned, previous studies described a number of conditions that give rise to paired nuclei in the *C. elegans* early embryo, including the down-regulation of RAB-5, which is involved in endocytosis (Audhya *et al.*, 2007), YOP-1 and RTN-1, which are involved in ER membrane tubulation (Audhya *et al.*, 2007), LPIN-1 (or lipin), a phosphatidic acid hydrolase that alters lipid composition and ER structure (Golden *et al.*, 2009; Gorjanacz and Mattaj, 2009), and CEPT-2, a choline/ethanolamine transferase (Bahmanyar *et al.*, 2014). In all cases, the paired-nuclei phenotype was associated with a defect in peripheral ER membrane organization (e.g., see the peripheral ER structure after *lpin-1* RNAi in Figure 10B and Supplemental Figure S5). In contrast, the peripheral ER of *plk-1*^{ts} embryos appeared morphologically normal (Figure 10A and Supplemental Figure S5), suggesting that partial inactivation of PLK-1 leads to a paired-nuclei phenotype through a distinct pathway. We did notice, however, abnormal membranous structures around centrosomes in *plk-1*^{ts} embryos. This membranous structure is distinct from the peripheral ER, as it contains NE proteins (Figure 10, C and D), which are not present in the peripheral ER. During mitosis in early wild-type embryos, centrosomes are surrounded by a membranous, ring-like structure that can be visualized with ER and certain NE markers (Poteryaev *et al.*, 2005; Morales-Martínez *et al.*, 2015). The organization of the membrane(s) in this structure is not known; for example, it may be composed of vesicles that may or may not be connected. We detected these structures using either LEM-2::GFP (Figure 9A, arrows) or SP12::GFP (Figure 10C, arrows), a lumenal ER marker. These ring-like structures are not a consequence of overexpression of these fluorescent proteins, as they were also observed when LEM-2::GFP was expressed at physiological levels (Morales-Martínez *et al.*, 2015). Although these structure appear to completely surround each centrosome, an opening must exist between each centrosome and the nucleus, as microtubules are able to access chromosomes and move them during prometaphase and anaphase. In *plk-1*^{ts} embryos, these ring-like structures were largely absent: in 11 of 18 embryos at metaphase, no rings were observed, and instead there were amorphous membranous structures (Figures 9B and 10D). In the remaining embryos, faint rings were observed either around both centrosomes (four of 11) or around only one centrosome (three of 11). Of interest, in other conditions noted earlier that resulted in paired nuclei, the ring-like structure around centrosomes appeared normal (Audhya *et al.*, 2007; Golden *et al.*, 2009; Gorjanacz and Mattaj, 2009). Thus the effect of PLK-1 on membrane organization is unique among known conditions that generate paired nuclei and appears to be confined to membranes surrounding the chromosomes and centrosomes.

The paired-nuclei phenotype caused by partial inactivation of PLK-1 can be suppressed by down-regulating certain NE components

If the underlying cause of the paired-nuclei phenotype is a defect in NEBD, then down-regulating certain NE components may suppress this phenotype. Such suppression could be due to a general weakening of the NE or the down-regulation of a PLK-1 substrate(s) that would normally be inactivated by PLK-1 phosphorylation. To examine whether down-regulation of certain NE proteins could suppress the paired-nuclei phenotype, we treated *plk-1*^{ts} animals with RNAi against various subunits of the NPC (NPP-1, NPP-2, etc.), the nuclear lamina (LMN-1 and LEM-2), and the LINC complex (SUN-1, ZYG-12, and ANC-1), which spans both nuclear membranes and links nuclear components with cytoskeletal elements (Tapley and Starr, 2013). As a control, we treated *plk-1*^{ts} animals with RNAi against SMD-1 (Golden *et al.*, 2009). The RNAi treatment, which was done by feeding worms bacteria that produce double-stranded RNA, was carried out at 23°C, and embryos up to

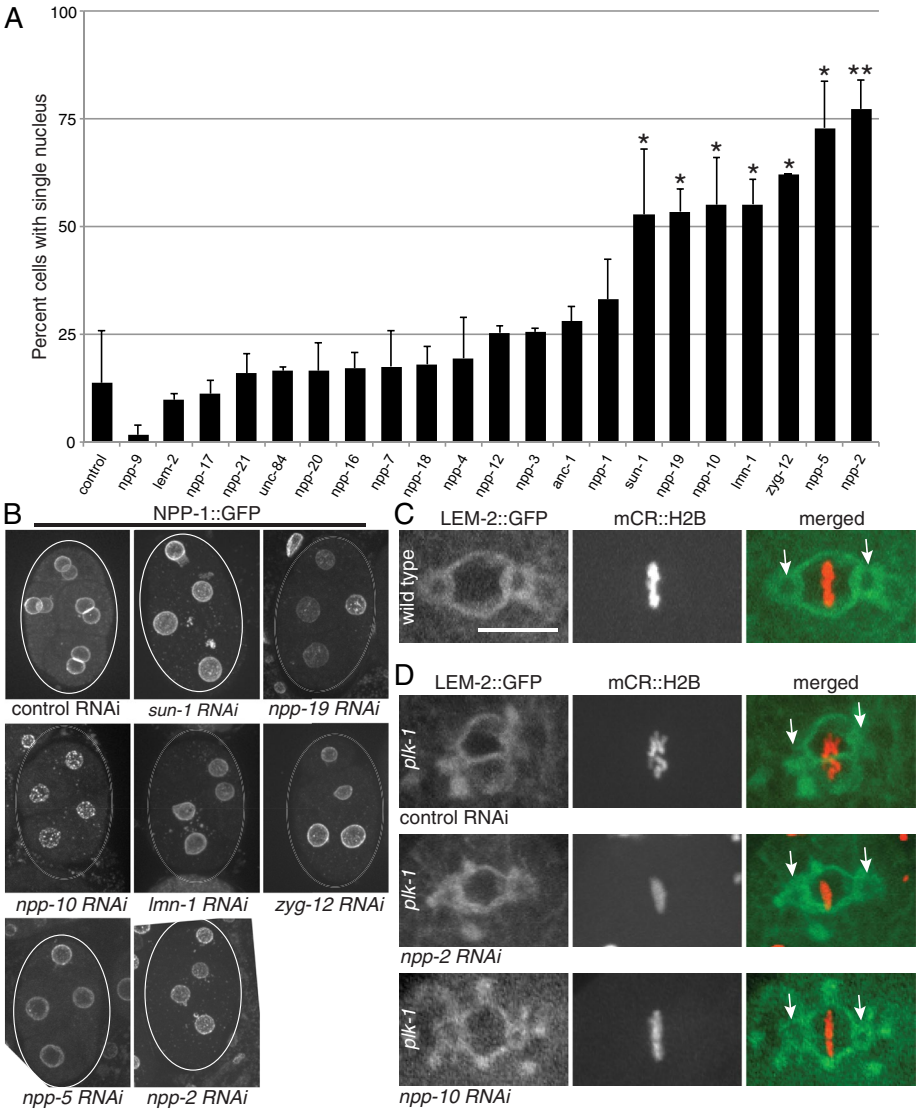

FIGURE 11: Down-regulation of certain NE components suppresses the paired-nuclei phenotype of *plk-1*^{ts}. (A) *plk-1*^{ts} hermaphrodites expressing NPP-1::GFP and mCherry H2B were treated with RNAi against the indicated NE components for 32 h at 23°C, and the percentage of cells with a single nucleus was scored in two- to 16-cell embryos. Error bars indicate SD based on data from multiple experiments (see *Materials and Methods*). Values that are statistically significantly different from the control (by Student's *t* test, $p < 0.05$) are marked by an asterisk. (B) Examples of four-cell *plk-1*^{ts} embryos from animals treated with the indicated RNAi as described in A. In some cases, the RNAi treatment led to an abnormal NPP-1::GFP pattern (see, e.g., *npp-10* RNAi). Bar, 10 µm. (C, D) Examples of metaphase configurations in one-cell wild-type (C) and *plk-1*^{ts} (D) embryos expressing LEM-2::GFP and mCherry::H2B. The *plk-1*^{ts} embryos were treated with RNAi against control, NPP-2, or NPP-10. Note the absence of NE marked by LEM-2::GFP between the maternal and paternal chromosomes after RNAi against NPP-2 or NPP-10 (D), resembling the wild-type situation (C). Also note the restoration of proper chromosome alignment and the partial restoration of ring-like structures at the spindle poles after the same two RNAi treatments (arrows). Bar, 10 µm.

the 16-cell stage were scored for the presence of cells with a single nucleus (Figure 11, A and B). In parallel, wild-type animals were exposed to RNAi against the same proteins to assess the effectiveness of the RNAi treatment (Supplemental Table S1). Of the 22 RNAi conditions tested, eight had no effect on the paired-nuclei phenotype or the viability of wild-type embryos, and thus it is not known whether the RNAi treatment was effective. Of the remaining RNAi treatments, a significant increase in the number of mononucleated cells was observed using RNAi against four NPC subunits—NPP-2 (homologous to human Nup85), NPP-5 (human Nup107), NPP-10 (human Nup96/98), and NPP-19 (human Nup53)—and against three nuclear lamina proteins—LMN-1 (human lamin B), SUN-1 (human SUN-domain proteins), and ZYG-12 (human KASH-domain proteins; Figure 11, A and B).

The presence of mononucleated cells is not sufficient to conclude that a true suppression of the paired-nuclei phenotype had taken place, namely that after pronuclear meeting, the NEs of the two pronuclei disassembled and the parental chromosomes intermingled. An alternative source of mononucleated cells in *plk-1*^{ts} embryos could be, for example, a failure of the pronuclei to meet, followed by cell division. This was a plausible explanation for the apparent suppression seen after RNAi treatment against ZYG-12 and SUN-1, as these proteins are needed for pronuclear movement after fertilization (Malone *et al.*, 2003). To determine whether the appearance of mononucleated cells reflected true suppression, we conducted time-lapse movies for all seven RNAi treatments that caused a significant increase in the percentage of mononucleated cells. In the case of RNAi against NPP-2, NPP-5, NPP-10, NPP-19, and LMN-1, the appearance of mononucleated cells was due to true suppression, namely the disassembly of the maternal and paternal NEs to form a single nucleus in the AB and P1 cells (Supplemental Figure S6, A–D). In contrast, RNAi treatment against ZYG-12 and the majority of RNAi treatments against SUN-1 caused a failure in pronuclear meeting, and when this was followed by nuclear division, the embryos contained one or two mononucleated cells (Supplemental Figure S6, E and F). In summary, down-regulation of certain NPC subunits or LMN-1 can suppress the paired-nuclear phenotype caused by the partial inactivation of PLK-1.

Of interest, RNAi against some of the aforementioned NPC subunits also resulted in significant restoration of the ring-like structures surrounding the centrosomes (Figure 11, C and D, and Supplemental Table S2). Even more striking, RNAi treatment against NPP-5 or NPP-10 restored normal chromosome congression and metaphase plate alignment in either all (in the case of *npp-5* RNAi) or a fraction (for *npp-10* RNAi) of mitoses in *plk-1*^{ts} embryos (Figure 11, C and D, and Supplemental Figure S7). The suppression of the paired-nuclei phenotype by RNAi against NPP-2 was not accompanied by a correction of the chromosome congression or metaphase plate alignment defect, suggesting that this suppression occurred via a different mechanism than the suppression by RNAi against NPP-5 and NPP-10. How down-regulation of certain NPC components can

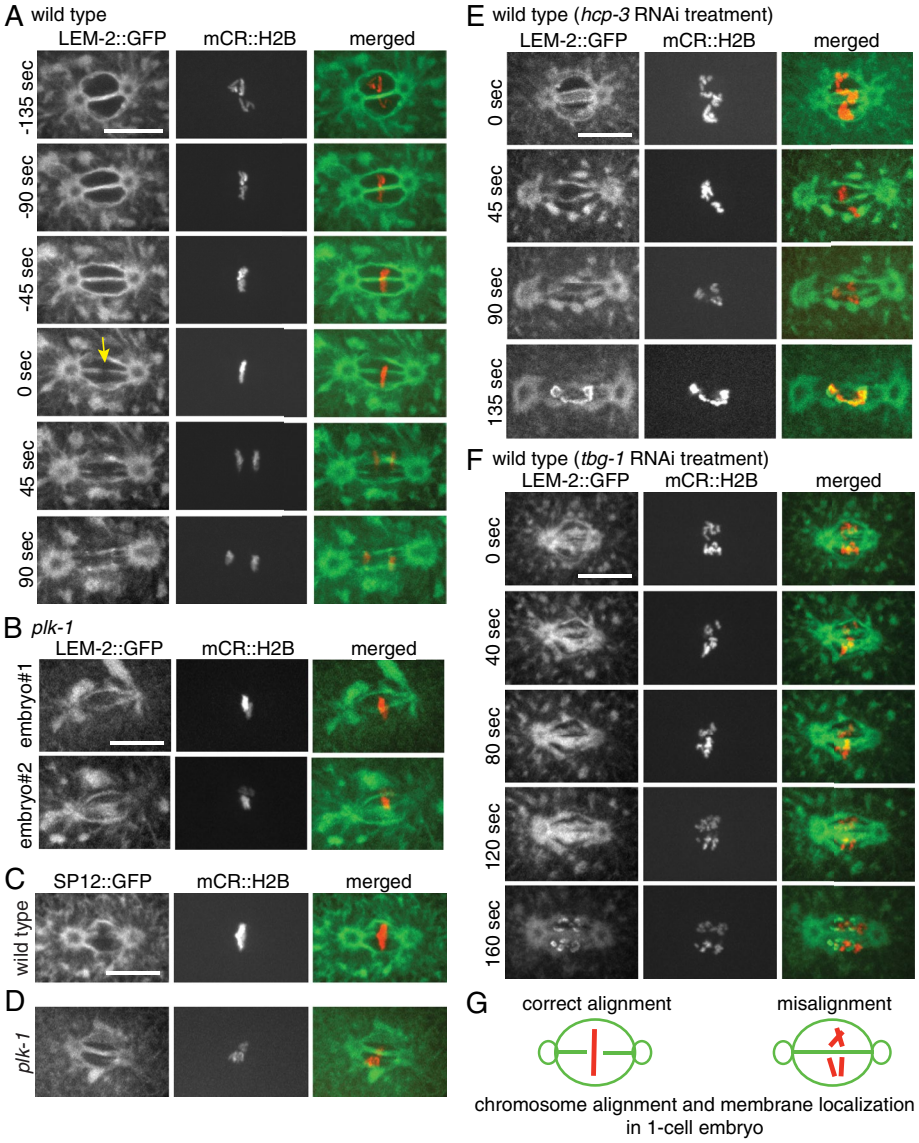

FIGURE 12: Chromosome congression and metaphase plate alignment precede membrane gap formation between the maternal and paternal chromosomes. (A) Time-lapse images of the NE and chromosomes in a wild-type one-cell embryo expressing LEM-2::GFP and mCherry::H2B. The completion of metaphase (namely, full chromosome congression and alignment of the maternal and paternal metaphase plates) was denoted as time $t = 0$ s. A gap appeared in the NE between the maternal and paternal chromosomes at time 0 s (arrow). This gap appeared in all LEM-2::GFP–expressing one-cell wild-type embryos as they completed metaphase ($n = 12$; see Supplemental Figure S6 for more examples). Bar, 10 μm. (B) Two examples of metaphase chromosomes and NE from *plk-1*^{ts} one-cell embryos expressing LEM-2::GFP and mCherry::H2B immediately before anaphase initiation. The NE between the maternal and paternal chromosomes persisted in all time-lapse movies analyzed ($n = 16$), all of which also showed defects in chromosome congression and/or metaphase plate alignment. Bar, 10 μm. (C, D) Representative example of chromosomes and NE from wild-type (C) and *plk-1*^{ts} (D) one-cell embryos expressing SP12::GFP and mCherry::H2B from time-lapse images immediately before anaphase. (E) Time-lapse images of chromosomes and NE of one-cell wild-type embryo treated with RNAi against HCP-3. In all cases in which metaphase plate formation failed, the NE between the maternal and paternal chromosomes persisted throughout mitosis ($n = 12$). Bar, 10 μm. (F) Time-lapse images of chromosomes and NE of one-cell wild-type embryo treated with RNAi against TBG-1 (γ-tubulin). In all cases in which metaphase plate formation failed, the NE between the maternal and paternal chromosomes persisted throughout mitosis ($n = 16$). Bar, 10 μm. (G) Cartoon representation of the NE (in green) and chromosomes (in red) at metaphase as observed in one-cell wild-type embryos (left) or under conditions in which chromosome congression and metaphase plate alignment are disrupted (right).

affect both the membrane around the centrosomes and congression/alignment is not known. Of interest, NPP-2, NPP-5, and the C-terminus of NPP-10 belong to the same NPC subcomplex—the NUP107 complex—that relocates from the NE to kinetochores during mitosis in worms and vertebrate cells and is required for proper kinetochore function (Loïodice *et al.*, 2004; Franz *et al.*, 2005; Ródenas *et al.*, 2012). In the *plk-1*^{ts} embryos, however, the localization of NPP-5 to the NE in interphase and kinetochores in mitosis appears normal (Supplemental Figure S8), indicating that the underlying chromosome alignment defect in *plk-1*^{ts} embryos is not due to the mislocalization of NPP-5 or the Nup107 complex. Furthermore, we could not detect abnormalities in *plk-1*^{ts} embryo spindle structure using immunofluorescence (M.M.R. and O.C.-F., unpublished data), but it is conceivable that the distorted membranous structures around centrosomes leads to subtle abnormalities in spindle structure or an alteration in spindle function. This, in turn, could cause a defect in chromosome congression and the alignment of the maternal and paternal metaphase plates.

Chromosome alignment is associated with NEBD between the maternal and paternal nuclei

Our data suggest that in one-cell embryos, there may be a link between the arrangement of maternal and paternal chromosomes in metaphase and the disassembly of the NEs between the two pronuclei. We therefore examined the configuration of chromosomes and the NE immediately before anaphase in wild-type cells, using time-lapse imaging of one-cell embryos expressing LEM-2::GFP and mCherry::H2B. As previously described (Audhya *et al.*, 2007), in wild-type one-cell embryos, chromosome congression and alignment of the maternal and paternal metaphase plates were coincident with the appearance of a gap in the NE between the two pronuclei (Figure 12A, $t = 0$ s, and Supplemental Figure S9). In fact, this gap appeared *only* once chromosome congression and metaphase plate alignment was achieved (see Supplemental Figure S9, embryo 3; notice the delay relative to embryos 1 and 2), suggesting a mechanism linking the completion of metaphase alignment to the formation of the membrane gap between the two pronuclei. The width of the gap increased as anaphase progressed (Figure 12A, $t = 45$ s). This gap was not seen in *plk-1*^{ts} one-cell embryos (Figure 12B; a gap was absent in 16 of 16 time-lapse movies analyzed), all of which also exhibited a

failure in chromosome congression and/or metaphase plate alignment. The presence of a gap in wild-type embryos and its absence in *plk-1*^{ts} embryos was also observed when using SP12::GFP, a lumenal ER marker (Figure 10, C and D).

If chromosome congression and/or metaphase plate alignment is needed for the formation of the gap, then other conditions that perturb this chromosome configuration in metaphase might also lead to a defect in gap formation. To test this, we down-regulated the centromere protein HCP-3 by RNAi. HCP-3 is the *C. elegans* homologue of CENP-A, a centromeric protein that is necessary for kinetochore assembly and hence the formation of chromosome-spindle microtubule attachments (Oegema *et al.*, 2001). Without these attachments, chromosomes cannot be moved properly in mitosis. Down-regulation of HCP-3 did not perturb the formation of ring-like structures around centrosomes (Figure 12E). However, down-regulation of HCP-3 abolished the formation of a gap in the NEs of the two pronuclei ($n = 6$; see, e.g., Figure 12E; the movement of centrosomes away from each other indicates that the cell is undergoing anaphase; compare the intercentrosomal distance at times 0 and 135 s), consistent with the requirement for chromosome congression for the formation of the membrane gap between the two pronuclei. Another way of perturbing metaphase plate formation in *C. elegans* is by down-regulating the γ-tubulin homologue TBG-1 using RNAi (Strome *et al.*, 2001). As the embryos underwent the first zygotic division, centrosomes moved apart in anaphase without chromosome alignment in metaphase, and the NE between the two pronuclei remained intact ($n = 16$; see, e.g., Figure 12F). Taken together, these results suggest that chromosome congression and the alignment of the two metaphase plates relative to each other are temporally linked to the formation of the gap between the maternal and paternal nuclei, which in turn leads to mixing of the two genomes after the first mitosis. In *plk-1*^{ts} embryos, as well as when HCP-3 and γ-tubulin are down-regulated, chromosomes do not achieve the required metaphase configuration, and we propose that, as a result, the NE between the maternal and paternal pronuclei remains intact in one-cell embryos. PLK-1 was previously shown to be involved in chromosome segregation (Sumara *et al.*, 2004; Park *et al.*, 2015), but whether it is also needed independently for the formation of the membrane gap itself is not known (see *Discussion*).

DISCUSSION

Previous analyses of PLK-1 function during *C. elegans* embryogenesis used depletion by RNAi, which led to complex phenotypes due to the requirement for PLK-1 in multiple processes (Chase *et al.*, 2000; Budirahardja and Gönczy, 2008; Nishi *et al.*, 2008; Noatynska *et al.*, 2013). Here, we took advantage of a *plk-1* temperature-sensitive allele, *or683ts*, and examined the consequences of partial inactivation of PLK-1 at a semipermissive temperature. Unlike partial inactivation by mild RNAi treatment, which often varies between individual animals and between experiments, exposure of the *plk-1*^{ts} animals to a semipermissive temperature resulted in a robust and highly reproducible phenotype. Under these conditions, meiosis, centrosome duplication, anaphase, and cytokinesis appeared largely unaffected, allowing us to uncover a highly penetrant defect in mixing of the maternal and paternal genomes after fertilization and a requirement for PLK-1 in NEBD in later embryonic divisions. Thus *C. elegans* embryos offer an excellent system in which to isolate PLK-1's function in NEBD from other PLK-1–dependent processes, allowing future research into the mechanism by which PLK-1 affects NEBD in worms and possibly vertebrates.

The origin of the defect in maternal and paternal chromosome mixing appeared to be the persistence of the NE of the two pronuclei: all three components of the NE that we examined—the NPC subunit NPP-1 and the nuclear lamina proteins LMN-1 and LEM-2—failed to dissociate from the NE during mitosis and persisted not only through the first cell division, but also in all subsequent divisions examined. Taken together, these data suggest that down-regulation of PLK-1 results in a NEBD defect. The resulting two nuclei in each daughter cell remained paired in interphase via an unknown mechanism. Clearly, some degree of NEBD in the vicinity of centrosomes must have occurred during mitosis, because the condensed chromosomes were moved by spindle microtubules, first toward a metaphase plate, albeit not perfectly (see later discussion), and then toward the spindle poles in anaphase. It is not known whether this partial NEBD, which is dependent on Aurora A and centrosomes (Portier *et al.*, 2007), is independent of PLK-1 function or whether at the semipermissive temperature there is sufficient residual PLK-1 activity to promote NEBD near the centrosomes. Nonetheless, when PLK-1 was partially inactivated, the NE between the maternal and paternal pronuclei remained intact throughout mitosis, precluding the mixing of the two genomes.

The possible involvement of Plk1 in NEBD in mammalian cells was suggested previously, based on Plk1 phosphorylation of proteins that are either part of the NE (e.g., Nup98; Laurell *et al.*, 2011) or contribute to NEBD (e.g., p150^{Glued}; Li *et al.*, 2010). However, in both cases, eliminating phosphorylation was insufficient to prevent NEBD. In *C. elegans*, down-regulation of PLK-1 by RNAi blocked NEBD in the oocyte (Chase *et al.*, 2000), but in that study, it was possible that one or more steps before NEBD failed to take place, thus inhibiting NEBD indirectly. Here we showed that when PLK-1 was partially inactivated, most processes associated with mitosis (e.g., centrosome duplication, chromosome segregation, cytokinesis) occurred normally, but certain aspects of NEBD were inhibited. Three lines of evidence suggest that PLK-1 contributes to complete NEBD after the one-cell stage: first, when *plk-1*^{ts} embryos were downshifted from the semipermissive (23°C) to the permissive (16°C) temperature, the paired-nuclei phenotype was largely resolved, yielding embryos with one nucleus per cell. Second, when *plk-1*^{ts} early embryos were shifted from the permissive to the semipermissive temperature, anaphase chromosomes became associated with NE, and NE was present between the two segregating DNA masses. Finally, persistence of NE components throughout mitosis was observed in a majority of P1 cells in wild-type two-cell embryos, for which PLK-1 levels are normally lower than in AB cells (Chase *et al.*, 2000; Budirahardja and Gönczy, 2008; Nishi *et al.*, 2008). Taken together, these findings suggest that under normal conditions, PLK-1 acts to completely disassemble the NE during early embryogenesis.

The permeability barrier of the NE is breached at a similar mitotic stage in both *C. elegans* early embryos and vertebrate cells, but the timing of nuclear lamina disassembly is later in *C. elegans* early embryos (namely, in metaphase/anaphase) than in vertebrates (in prophase/prometaphase). One could have argued that in *C. elegans*, once the NE is permeabilized, all other aspects associated with NEBD are unimportant and the complete disassembly of the nuclear lamina is merely "cosmetic." In fact, we show that when PLK-1 is down-regulated after the first mitosis, cells can undergo chromosome segregation and cell division with a partially disassembled NE. However, we also show that lamina disassembly during metaphase is essential during the first embryonic mitosis, as the persistence of a nuclear lamina between the two pronuclei in the *plk-1* mutant blocked mixing of the parental genome, whereas down-regulation of *lmn-1* suppressed this phenotype. This suggests that, at least in the one-cell stage, breaching the NE permeability barrier is not sufficient and that complete NEBD, including lamina disassembly, is required. Moreover, in our temperature up-shift experiment, incomplete NEBD

resulted in the formation of cytoplasmic foci containing NPCs. Although we do not know what effect, if any, these foci have on the cell, their presence is certainly abnormal. In vertebrates, NEBD is largely driven by Cdk1 (for review, see Álvarez-Fernández and Malumbres, 2014), and lamina disassembly can be blocked by mutating certain Cdk1 phosphorylation sites (Heald and McKeon, 1990). We postulate that if Plk1 contributes to vertebrate NEBD in a process that peaks at metaphase/anaphase, its requirement would be largely masked by Cdk1 activity that drives all aspects of NEBD, including lamina disassembly, as early as prophase. The disassembly of the *C. elegans* early-embryo lamina in metaphase/anaphase coincides with a decline in Cdk1 activity owing to APC/C activity (van der Voet *et al.*, 2009). Thus we hypothesize that in *C. elegans* early embryos, lamina disassembly is refractory to Cdk1 activity and instead is largely driven by PLK-1. The unique behavior of the NE in the *C. elegans* early embryo allowed us to uncover a Plk1-dependent NEBD process that may also be relevant to NEBD in vertebrates.

In wild-type *C. elegans* embryos, after pronuclear meeting, the maternal and paternal chromosomes align on their respective metaphase plates, the two metaphase plates align relative to each other, a membrane gap forms in the NEs between the two pronuclei, the space between the two genomes disappears, and anaphase ensues. We observed that the gap in the NE formed only when the chromosomes of the two pronuclei were fully congressed on their respective metaphase plates and the metaphase plates were aligned relative to each other. Of note, under conditions in which this chromosome configuration was not achieved, such as partial inactivation of PLK-1, down-regulation of the centromeric protein HCP-3, or down-regulation of γ-tubulin, the gap in the NE between the two pronuclei did not form, resulting in a failure to mix the parental chromosomes. Furthermore, conditions that suppressed the paired-nuclei phenotype, namely down-regulation of the NPP-5 and NPP-10 NPC subunits, also suppressed the chromosome alignment defect. We speculate that the defect in chromosome alignment after partial inactivation of PLK-1 is functionally linked to the defect in NE gap formation between the two pronuclei. Because PLK-1 is associated with chromosomes until anaphase initiation (Nishi *et al.*, 2008), it is possible that the alignment of the chromosomes creates a critical localized concentration of PLK-1 or its substrate(s) at the NE between the two metaphase plates, leading to gap formation. Alternatively, PLK-1 could affect NEBD indirectly, by contributing to chromosome alignment, which, in turn, signals formation of the gap. PLK-1 is likely to have a more direct role in the disassembly of NE components beyond the formation of the gap between the two pronuclei because when PLK-1 is partially inactivated, components of the NE around the entirety of each pronucleus, and around nuclei later in embryogenesis, fail to disassemble.

How might PLK-1 affect NEBD? Biochemical, phosphoproteomic, and computational analyses, mostly in animal cells, have revealed that many NPC subunits are targets of Plk1, including Nup53/Nup35, Nup85, Nup88, Nup93, Nup98, Nup107, Nup33, Nup153, Nup160, Nup205, and TPR (Santamaria *et al.*, 2010; Grosstessner-Hain *et al.*, 2011; Hegemann *et al.*, 2011; Kettenbach *et al.*, 2011; Bibi *et al.*, 2013). Lamin B1 was also phosphorylated by Plk1 (Kettenbach *et al.*, 2011). With the exception of Nup88, all of these NPC subunits have homologues in *C. elegans*. Of interest, we observed that down-regulation of Nup85 (*C. elegans* NPP-2), Nup107 (NPP-5), Nup96/98 (NPP-10), and Nup53/35 (NPP-19) suppressed the paired- nuclei phenotype of *plk-1^{ts}* embryos. The most straightforward interpretation of this result is that PLK-1 normally weakens the NE by phosphorylating one of more NPC subunit, and down-regulation of certain NPC subunits phenocopies this process. However, it is also possible, based on our data, that gap formation between the two pronuclei could be dependent on proper chromosome configuration during metaphase, and we note that two of the suppressing RNAi treatments that resolved the paired-nuclei phenotype also corrected *the plk-1^{ts}* chromosome congression and metaphase plate alignment defect. Because Plk1 is known to play a role in kinetochore–microtubule attachments (Sumara *et al.*, 2004), we speculate that the suppression by down-regulating NPP-5 or NPP-10, which are components of the Nup107 complex that localizes to kinetochores during mitosis, is mediated by the restoration of chromosome alignment.

NPP-2 is also part of the Nup107 complex, but *npp-2* RNAi suppressed the paired-nuclei phenotype without correcting the chromosome alignment defect. Formally, there could be two explanations for the difference between *npp-5/npp-10* RNAi and *npp-2* RNAi. First, suppressors can reverse a mutant phenotype by affecting different parts of a pathway. In our case, RNAi against NPP-5 and NPP-10 may have resolved the underlying defect, whereas RNAi against NPP-2 targeted either a more downstream part of the pathway or acted through a different pathway, correcting the paired-nuclei phenotype without affecting the chromosome alignment defects. Of note, in a previous study, the phenotype caused by RNAi against NPP-2 was somewhat different from that caused by RNAi against NPP-10 (Ródenas *et al.*, 2012). Alternatively, all three RNAi treatments correct the paired-nuclei phenotype through a mechanism unrelated to chromosome alignment, and the differences in the phenotypes conferred by the three RNAi treatments may be a result of different RNAi efficiencies. Either way, elucidating the mechanism of suppression will shed light on the processes that lead to NEBD between the two pronuclei.

The formation of paired nuclei was previously observed after conditions that altered peripheral ER structure (Audhya *et al.*, 2007; Golden *et al.*, 2009; Gorjanacz and Mattaj, 2009; Bahmanyar *et al.*, 2014) and down-regulation of gp210, an NPC subunit (Audhya *et al.*, 2007; Galy *et al.*, 2008). Parenthetically, in some of these studies, paired nuclei were referred to as "twinned nuclei." We favor the term "paired nuclei," as "twinned" implies a genetic identity of the two nuclei (e.g., siblings), unlike maternal and paternal pronuclei, which are genetically distinct. Our data suggest that PLK-1 affects NEBD through a pathway unrelated to peripheral ER structure or gp210: partial inactivation of PLK-1 did not markedly affect peripheral ER structure, nor did it affect gp210 localization or levels (Supplemental Figure S10), which might have phenocopied gp210 down-regulation. Moreover, the paired-nuclei phenotype in *plk-1^{ts}* embryos extended through many cell divisions, whereas that of gp210 inactivation was largely resolved after the first cell division (Galy *et al.*, 2008). Finally, unlike *plk-1^{ts}* embryos, when RAB-5 or LPIN-1 were down-regulated, peripheral ER structure was altered, but the ring-like structures around the centrosomes formed normally (Audhya *et al.*, 2007; Gorjanacz and Mattaj, 2009). In addition, we did not observe an extra layer of ER around the nucleus in *plk-1^{ts}* embryos, which was seen after down-regulation of a LPIN-1 activator (Bahmanyar *et al.*, 2014). Rather than affecting the peripheral ER, our data are consistent with a mechanism linking NEBD between the two pronuclei to chromosome congression and the alignment of the maternal and paternal metaphase plates. The role played by PLK-1 in this process, whether it merely contributes to chromosome configuration or plays a more direct role in creating a fenestration in the two NEs remains to be discovered.

The temporal coupling between chromosome alignment and the formation of a membrane gap in the NEs of the two pronuclei is reminiscent of a checkpoint mechanism that links the completion of one process to the execution of a subsequent one (Hartwell and Weinert, 1989). Alternatively, the precise chromosome configuration

at the time of membrane gap formation may create a critical concentration of a chromosome-associated factor(s) needed for the formation of this gap. An interesting question is the structure of the gap, which has to traverse the four membranes that make up the two pronuclear NEs. A similar situation occurs during the first mitotic division in *Drosophila*, where the NE prevents intermingling of maternal and paternal chromosome until telophase, when presumably the NE between the two pronuclei is breached (Callaini and Riparbelli, 1996). In both cases, the nuclear membranes of both pronuclei must somehow fuse and then retract during either anaphase (*C. elegans*) or telophase (*Drosophila*). A potentially analogous membrane fusion event occurs during budding yeast mating, when two haploid cells, and their nuclei, fuse to give rise to a diploid zygote (Melloy *et al.*, 2007). In this case, the fusion of the two nuclei occurs in two steps: initially, the outer nuclear membranes of the two nuclei fuse, followed by fusion of the two inner nuclear membranes. Whether an analogous process occurs during zygote formation in *C. elegans*, and perhaps in other metazoans, awaits further investigations.

MATERIALS AND METHODS

Strains

C. elegans strains were maintained at the permissive temperature using standard methods (Brenner, 1974), except where noted otherwise. For all experiments in which paired nuclei and accompanying phenotypes were analyzed, strains were incubated at 23°C unless otherwise noted. A list of *C. elegans* strains and their genotypes is provided in Supplemental Table S3.

Temperature shift experiments

For temperature down-shift experiments, embryos from *plk-1*^{ts} animals expressing LEM-2::GFP were laid at 23°C and then shifted to 16°C for 3 h. Embryos were imaged before and after the temperature shift. For temperature up-shift experiments, wild-type and *plk-1*^{ts} homozygous animals expressing mCherry::histone H2B and NPP-1::GFP were maintained at 16°C. Gravid adult animals were collected, dissected on a coverslip, and placed on 2% agarose pads. Early- stage (two-cell, four-cell, or eight-cell) embryos were identified under the microscope, imaged, and immediately transferred to 23°C. The same embryos were examined after 2.5 h of incubation at 23°C, and the state of the NE in anaphase cells was quantified.

RNAi experiments

All feeding RNAi constructs were obtained from the Open Biosystems RNAi library (Huntsville, AL). Feeding RNAi was performed using a standard feeding method (Kamath and Ahringer, 2003). The identity of each RNAi clone was verified by sequencing. For each suppression experiment, 15–20 L4-stage *plk-1*^{ts} larvae were transferred to RNAi plates, and 30–40 embryos were examined after 32 h of RNAi treatment at 23°C. RNAi experiments were done blind, and the identity of the RNAi treatment was revealed only after the phenotypic scoring was completed. For each treatment, at least 15 animals were collected for scoring embryos, and each experiment was repeated at least four to six times. To determine embryonic lethality, 10 wild-type animals were grown on RNAi plates of the same batch as the suppression experiment, transferred to a new plate after 32 h of RNAi treatment, and removed 1–2 h after egg-laying commenced. Hatching was scored 24 h later.

For the *par* RNAi and *tbg*-1 RNAi experiments, bacterial cultures containing the appropriate RNAi vectors against PAR-1, PAR-2, and PAR-5 were grown overnight at 37°C, diluted 100-fold, and grown to an OD_{600} of 0.3–0.4. At this point, isopropyl-β-D-thiogalactoside (IPTG) was added to a final concentration of 0.5 mM and cultures grown for an additional 6 h, as described previously (Timmons *et al.*, 2001). Equal volumes of the three *par* RNAi cultures were mixed, plated on an IPTG plate, and allowed to dry at room temperature.

Microscopy and image processing

With the exception of the images in Figure 6, confocal images of live embryos were taken using a Nikon Eclipse TE2000U spinning-disk confocal microscope with IPLab 4.0.8 (BioVision Technologies, Exton, PA) or MetaMorph 7.8.8.0 (Molecular Devices, Sunnyvale, CA) software. The microscope was equipped with a 60×/1.4 numerical aperture (NA) Apo objective, four LMM5 laser merge module with diode lasers (excitation at 405, 491, 561, and 655 nm) from Applied Research, a CSU10 spinning-disk unit by Yokogawa, and a C9100-13 electron-multiplying charge-coupled device camera by Hamamatsu. For live-cell imaging, three or four animals were placed in a drop of 20 mM freshly prepared levamisole hydrochloride (MP Biomedicals, Santa Ana, CA) aqueous solution. Animals were cut open on a 22-mm-square coverglass (thickness no. 1; Corning, Corning, NY) with a 22-gauge needle to release the embryos and mounted on a 2% agarose pad. Embryos were imaged using a *Z*-step of 1 µm, acquiring images using the 491-nm laser and then the 561-nm laser. Images were processed with IPLab 4.0.8, MetaMorph 7.8.8.0, ImageJ 1.44o (National Institutes of Health, Bethesda, MD), Adobe Photoshop CS6, version 13.0.6, and Adobe Illustrator CS5, version 15.1.0.

Immunocytochemistry and quantification of the H3K27me3 pattern

We mated *fog-1; plk-1* feminized L4 hermaphrodites for ~20 h at 23°C either to N2 males to generate *plk-1*/+ embryos or to *mes-3* males to generate *plk-1/+; mes-3/+* M+P– embryos. Embryos were dissected from mated females in egg buffer (25 mM 4-(2-hydroxyethyl)-1-piperazineethanesulfonic acid, pH 7.4, 118 mM NaCl, 48 mM KCl, 2 mM $MgCl_2$) containing 1 mM levamisole, fixed using methanol/acetone, and stained (Strome and Wood, 1983). Primary antibodies and dilutions used for immunostaining were 1:30,000 mouse anti-H3K27me3 (39535; Active Motif, Carlsbad, CA) and 1:10,000 rabbit anti-H3K4me2 (07030; Millipore, Billerica, MA). Primary antibodies were incubated overnight at 4°C. Secondary goat anti-mouse antibodies conjugated to Alexa Fluor 488 and goat anti-rabbit conjugated to Alexa Fluor 594 (Molecular Probes, Eugene, OR) were used at 1:300 with 0.05 µg/ml 4′,6-diamidino-2-phenylindole for 2 h at room temperature. Images were acquired with a Volocity spinning-disk confocal system (PerkinElmer/ImproVision, Norwalk, CT) fitted on a Nikon Eclipse TE2000-E inverted microscope. To quantify the paired nuclei and H3K4me2 versus H3K27me3 staining, embryos were fixed and stained as described. Stacks of optical sections were collected with the described spinning-disk microscope. Sixteen embryos between the two- and 12-cell stage were scored for the number of cells with a pair of nuclei and for the number of nuclei that contained H3K27me3. Analysis was focused on embryos presumed to be XO males, as embryos presumed to be XX hermaphrodites contained an H3K27me3-stained chromosome, likely the sperm-contributed X, in the paternal set of chromosomes. All cells with the exception of cells in metaphase were scored. Of 91 cells, 85 (93%) contained a pair of nuclei. Of those 85 cells with a pair of nuclei, 100% displayed H3K27me3 in only one nucleus of the pair, whereas H3K4me2 was observed in both nuclei.

High-pressure freezing and transmission electron microscopy

Early embryos were collected in capillary tubing and cryoimmobilized using an EMPACT2+RTS high-pressure freezer (Leica

Microsystems, Wetzlar, Germany). Samples were freeze substituted at −90°C for 48 h in acetone containing 1% osmium tetroxide and 0.1% uranyl acetate. The temperature was raised progressively to room temperature in an automatic freeze-substitution machine (Leica EM AFS, Wetzlar, Germany), and samples were thin-layer embedded in Epon/Araldite as published (Pelletier *et al.*, 2006; Müller-Reichert *et al.*, 2007). Thin sections (70 nm) were cut using a Leica Ultracut UCT microtome and collected on Formvar-coated copper grids. Sections were poststained with 2% uranyl acetate in 70% methanol, followed by aqueous lead citrate and viewed in either a TECNAI 12 (FEI, Hillsboro, OR) or EM 906 (Zeiss, Oberkochen, Germany) transmission electron microscope operated at 80 and 120 kV, respectively. To calculate the distance between the paired nuclei in the serial sections shown in Figure 2, three measurements were taken for each slice at the closest points between the paired nuclei, and the average value is depicted in the graph. Of note, at no point was the distance between the paired nuclei close to 0.

ACKNOWLEDGMENTS

We thank Kevin O'Connell for alerting us to the *plk-1(or683ts)* mutant phenotype and members of the O'Connell, Golden, and Cohen-Fix labs for advice. We also thank Andy Golden, Ally Walters, Simona Rosu, and Harold Smith for excellent comments on the manuscript. T.M.-R. was funded by the Deutsche Forschungsgemeinschaft (DFG SPP1384, Grant MU1423/3-1 and 3-2). K.K. and S.S. were funded by National Institutes of Health R01 Grant GM34059. M.M.R., B.L., and O.C.-F. were funded by an intramural grant from the National Institute of Diabetes and Digestive and Kidney Diseases/National Institutes of Health.

REFERENCES

Abrieu A, Brassac T, Galas S, Fisher D, Labbe JC, Doree M (1998). The polo-like kinase Plx1 is a component of the MPF amplification loop at the G(2)/M-phase transition of the cell cycle in Xenopus eggs. J Cell Sci 111, 1751–1757.

Álvarez-Fernández M, Malumbres M (2014). Preparing a cell for nuclear envelope breakdown: Spatio-temporal control of phosphorylation during mitotic entry. Bioessays 36, 757–765.

Amendola M, van Steensel B (2014). Mechanisms and dynamics of nuclear lamina. Curr Opin Cell Biol 28, 61–68.

Archambault V, Glover DM (2009). Polo-like kinases: conservation and divergence in their functions and regulation. Nat Rev Mol Cell Biol 10, 265–275.

Askjaer P, Galy V, Hannak E, Mattaj IW (2002). Ran GTPase cycle and importins α and β are essential for spindle formation and nuclear envelope assembly in living *Caenorhabditis elegans* embryos. Mol Biol Cell 13, 4335-4370.

Audhya A, Desai A, Oegema K (2007). A role for Rab5 in structuring the endoplasmic reticulum. J Cell Biol 178, 43–56.

Bahmanyar S, Biggs R, Schuh AL, Desai A, Muller-Reichert T, Audhya A, Dixon JE, Oegema K (2014). Spatial control of phospholipid flux restricts endoplasmic reticulum sheet formation to allow nuclear envelope breakdown. Genes Dev 28, 121–126.

Baran V, Solc P, Kovarikova V, Rehak P, Sutovsky P (2013). Polo-like kinase 1 is essential for the first mitotic division in the mouse embryo. Mol Reprod Dev 80, 522–534.

Beaudouin J, Gerlich D, Daigle N, Eils R, Ellenberg J (2002). Nuclear envelope breakdown proceeds by microtubule-induced tearing of the lamina. Cell 108, 83–96.

Bender LB, Cao R, Zhang Y, Strome S (2004). The MES-2/MES-3/MES-6 complex and regulation of histone H3 methylation in C. elegans. Curr Biol 14, 1639–1643.

Bibi N, Parveen Z, Rashid S (2013). Identification of potential Plk1 targets in a cell-cycle specific proteome through structural dynamics of kinase and polo box-mediated interactions. PLoS One 8, e70843.

Brachner A, Reipert S, Foisner R, Gotzmann J (2005). LEM2 is a novel MAN1-related inner nuclear membrane protein associated with A-type lamins. J Cell Sci 118, 5797–5810.

Brenner S (1974). The genetics of Caenorhabditis elegans. Genetics 77, 71–94.

Budirahardja Y, Gönczy P (2008). PLK-1 asymmetry contributes to asynchronous cell division of C. elegans embryos. Development 135, 1303–1313.

Burke B, Stewart CL (2013). The nuclear lamins: flexibility in function. Nat Rev Mol Cell Biol 14, 13–24.

Callaini G, Riparbelli MG (1996). Fertilization in Drosophila melanogaster: centrosome inheritance and organization of the first mitotic spindle. Dev Biol 176, 199–208.

Capowski EE, Martin P, Garvin C, Strome S (1991). Identification of grandchildless loci whose products are required for normal germ-line development in the nematode Caenorhabditis elegans. Genetics 129, 1061–1072.

Chase D, Serafinas C, Ashcroft N, Kosinski M, Longo D, Ferris DK, Golden A (2000). The polo-like kinase PLK-1 is required for nuclear envelope breakdown and the completion of meiosis in Caenorhabditis elegans. Genesis 26, 26–41.

Dessev G, Iovcheva-Dessev C, Bischoff JR, Beach D, Goldman R (1991). A complex containing p34cdc2 and cyclin B phosphorylates the nuclear lamin and disassembles nuclei of clam oocytes in vitro. J Cell Biol 112, 523-533.

Franz C, Askjaer P, Antonin W, Iglesias CL, Haselmann U, Schelder M, de Marco A, Wilm M, Antony C, Mattaj IW (2005). Nup155 regulates nuclear envelope and nuclear pore complex formation in nematodes and vertebrates. EMBO J 24, 3519–3531.

Galy V, Antonin W, Jaedicke A, Sachse M, Santarella R, Haselmann U, Mattaj I (2008). A role for gp210 in mitotic nuclear-envelope breakdown. J Cell Sci 121, 317–328.

Galy V, Askjaer P, Franz C, López-Iglesias C, Mattaj IW (2006). MEL-28, a novel nuclear-envelope and kinetochore protein essential for zygotic nuclear-envelope assembly in C. elegans. Curr Biol 16, 1748–1756.

Gaydos LJ, Wang W, Strome S (2014). H3K27me and PRC2 transmit a memory of repression across generations and during development. Science 345, 1515–1518.

Golden A, Liu J, Cohen-Fix O (2009). Inactivation of the C. elegans lipin homolog leads to ER disorganization and to defects in the breakdown and reassembly of the nuclear envelope. J Cell Sci 122, 1970–1978.

Gönczy P, Rose LS (2005). Asymmetric cell division and axis formation in the embryo. WormBook 2005(Oct 15), 1–20.

Gönczy P, Schnabel H, Kaletta T, Amores AD, Hyman T, Schnabel R (1999). Dissection of cell division processes in the one cell stage Caenorhabditis elegans embryo by mutational analysis. J Cell Biol 144, 927–946.

Gondos B, Bhiraleus P, Conner LA (1972). Pronuclear membrane alterations during approximation of pronuclei and initiation of cleavage in rabbit. J Cell Sci 10, 61–78.

Gorjánácz M, Klerkx EPF, Galy V, Santarella R, López-Iglesias C, Askjaer P, Mattaj IW (2007). Caenorhabditis elegans BAF-1 and its kinase VRK-1 participate directly in post-mitotic nuclear envelope assembly. EMBO J 26, 132–143.

Gorjanacz M, Mattaj IW (2009). Lipin is required for efficient breakdown of the nuclear envelope in Caenorhabditis elegans. J Cell Sci 122, 1963–1969.

Grosstessner-Hain K, Hegemann B, Novatchkova M, Rameseder J, Joughin BA, Hudecz O, Roitinger E, Pichler P, Kraut N, Yaffe MB, *et al.* (2011). Quantitative phospho-proteomics to investigate the polo-like kinase 1-dependent phospho-proteome. Mol Cell Prot 10, M111.008540.

Güttinger S, Laurell E, Kutay U (2009). Orchestrating nuclear envelope disassembly and reassembly during mitosis. Nat Rev Mol Cell Biol 10, 178–191.

Hachet V, Busso C, Toya M, Sugimoto A, Askjaer P, Gönczy P (2012). The nucleoporin Nup205/NPP-3 is lost near centrosomes at mitotic onset and can modulate the timing of this process in Caenorhabditis elegans embryos. Mol Biol Cell 23, 3111–3121.

Hachet V, Canard C, Gönczy P (2007). Centrosomes promote timely mitotic entry in *C. elegans* embryos. Dev Cell 12, 531–541.

Hartwell LH, Weinert TA (1989). Checkpoints: controls that ensure the order of cell cycle events. Science 246, 629–634.

Hayashi H, Kimura K, Kimura A (2012). Localized accumulation of tubulin during semi-open mitosis in the *Caenorhabditis elegans* embryo. Mol Biol Cell 23, 1688-1699.

Heald R, McKeon F (1990). Mutations of phosphorylation sites in Lamin A that prevent nuclear lamina disassembly in mitosis. Cell 61, 579-589.

Hegemann B, Hutchins JRA, Hudecz O, Novatchkova M, Rameseder J, Sykora MM, Liu S, Mazanek M, Lenart P, Heriche J, *et al.* (2011). Systematic phosphorylation analysis of human mitotic protein complexes. Sci Signal 4, rs12.

Iwamatsu T, Kobayashi H (2002). Electron microscopic observations of karyogamy in the fish egg. Dev Growth Differ 44, 357–363.

Kamath RS, Ahringer J (2003). Genome-wide RNAi screening in Caenorhabditis elegans. Methods 30, 313–321.
Katsani KR, Karess RE, Dostatni N, Doye V (2008). In vivo dynamics of Drosophila nuclear envelope components. Mol Biol Cell 19, 3652–3666.
Kettenbach AN, Schweppe DK, Faherty BK, Pechenick D, Pletnev AA, Gerber SA (2011). Quantitative phosphoproteomics identifies substrates and functional modules of Aurora and polo-like kinase activities in mitotic cells. Sci Signal 4, rs5.
Kitada K, Johnson AL, Johnson LH, Sugino A (1993). A multicopy suppressor gene of the Saccharomyces-crevisiae G1 cell-cycle mutant-gene Dbf4 encodes a protein-kinase and is identified as Cdc5. Mol Cell Biol 13, 4445–4457.
Laurell E, Beck K, Krupina K, Theerthagiri G, Bodenmiller B, Horvath P, Aebersold R, Antonin W, Kutay U (2011). Phosphorylation of Nup98 by multiple kinases is crucial for NPC disassembly during mitotic entry. Cell 144, 539–550.
Lee KK, Gruenbaum Y, Spann P, Liu J, Wilson KL (2000). C. elegans nuclear envelope proteins emerin, MAN1, lamin, and nucleoporins reveal unique timing of nuclear envelope breakdown during mitosis. Mol Biol Cell 11, 3089–3099.
Lénárt P, Peters JM (2006). Checkpoint activation: don't get mad too much. Curr Biol 16, R412–R414.
Lénárt P, Petronczki M, Steegmaier M, Fiore BD, Lipp JJ, Hoffman M, Rettig WJ, Kraut N, Peters JM (2007). The small-molecule inhibitor BI2536 reveals novel insights into mitotic roles of Polo-like kinase 1. Curr Biol 17, 304-315.
Levron J, Munne S, Willadsen S, Rosenwaks Z, Cohen J (1995). Male and female genomes associated in a single pronucleus in human zygotes. Biol Reprod 52, 653–657.
Li H, Liu XS, Yang X, Song B, Wang Y, Liu X (2010). Polo-like kinase 1 phosphorylation of p150Glued facilitates nuclear envelope breakdown during prophase. Proc Natl Acad Sci USA 107, 14633–14638.
Loïodice I, Alves A, Rabut G, van Overbeek M, Ellenberg J, Sibarita JB, Doye V (2004). The entire Nup107-160 complex, including three new members, is targeted as one entity to kinetochores in mitosis. Mol Biol Cell 15, 3333–3344.
Malone CJ, Misner L, Le Bot N, Tsai MC, Campbell JM, Ahringer J, White JG (2003). The C. elegans hook protein, ZYG-12, mediates the essential attachment between the centrosome and nucleus. Cell 115, 825–836.
Melloy P, Shen S, White E, Mcintosh JR, Rose MD (2007). Nuclear fusion during yeast mating occurs by a three-step pathway. J Cell Biol 179, 659–670.
Molitor TP, Traktman P (2014). Depletion of the protein kinase VRK1 disrupts nuclear envelope morphology and leads to BAF retention on mitotic chromosomes. Mol Biol Cell 25, 891–903.
Morales-Martínez A, Dobrzynska A, Askjaer P (2015). Inner nuclear membrane protein LEM-2 is required for correct nuclear separation and morphology in C. elegans. J Cell Sci 128, 1090–1096.
Müller-Reichert T, Srayko M, Hyman A, O'Toole ET, McDonald K (2007). correlative light and electron microscopy of early Caenorhabditis elegans embryos in mitosis. In: Cellular Electron Microscopy, ed. J McIntosh, New York: Elsevier, 101–119.
Nishi Y, Rogers E, Robertson SM, Lin R (2008). Polo kinases regulate C. elegans embryonic polarity via binding to DYRK2-primed MEX-5 and MEX-6. Development 135, 687–697.
Noatynska A, Panbianco C, Gotta M (2010). SPAT-1/Bora acts with Polo-like kinase 1 to regulate PAR polarity and cell cycle progression. Development 137, 3315–3325.
Noatynska A, Tavernier N, Gotta M, Pintard L (2013). Coordinating cell polarity and cell cycle progression: what can we learn from flies and worms? Open Biol 3, 130083.
Oegema J, Desai A, Rybina S, Kirkham M, Hyman AA (2001). Functional analysis of kinetochore assembly in Caenorhabditis elegans. J Cell Biol 153, 1209–1226.
O'Rourke SM, Carter C, Carter L, Christensen SN, Jones MP, Nash B, Price MH, Turnbull DW, Garner AR, Hamill DR, *et al*. (2011). A survey of new temperature-sensitive, embryonic-lethal mutations in C. elegans: 24 alleles of thirteen genes. PLoS One 6, e16644.
Paddy MR, Saumweber H, Agard DA, Sedat JW (1996). Time-resolved, in vivo studies of mitotic spindle formation and nuclear lamina breakdown in *Drosophila* early embryos. J Cell Sci 109, 591-607.
Park CH, Park JE, Kim TS, Kang YH, Soung NK, Zhou M, Kim NH, Bang JK, Lee KS (2015). Mammalian polo-like kinase 1 (Plk1) promotes proper chromosome segregation by phosphorylating and delocalizing the PBIP1·CENP-Q Complex from kinetochores. J Biol Chem 290, 8569–8581.
Pelletier L, O'Toole E, Schwager A, Hyman AA, Müller-Reichert T (2006). Centriole assembly in Caenorhabditis elegans. Nature 444, 619–623.
Peter M, Nakagawa J, Doree M, Labbe JC, Nigg EA (1990). In vitro disassembly of the nuclear lamina and M phase-specific phosphorylation of lamins by cdc2 kinase. Cell 61, 591–602.
Petronczki M, Glotzer M, Kraut N, Peters JM (2007). Polo-like kinase 1 triggers the initiation of cytokinesis in human cells by promoting recruitment of the RhoGEF Ect2 to central spindle. Dev Cell 12, 713–725.
Petronczki M, Lénárt P, Peters JM (2008). Polo on the rise—from mitotic entry to cytokinesis with Plk1. Dev Cell 14, 646–659.
Portier N, Audhya A, Maddox PS, Green RA, Dammermann A, Desai A, Oegema K (2007). A microtubule-independent role for centrosomes and aurora a in nuclear envelope breakdown. Dev Cell 12, 515–529.
Poteryaev D, Squirrell JM, Campbell JM, White JG, Spang A (2005). Involvement of the actin cytoskeleton and homotypic membrane fusion in ER dynamics in Caenorhabditis elegans. Mol Biol Cell 16, 2139–2153.
Rivers DM, Moreno S, Abraham M, Ahringer J (2008). PAR proteins direct asymmetry of the cell cycle regulators Polo-like kinase and Cdc25. J Cell Biol 180, 877–885.
Ródenas E, González-Aguilera C, Ayuso C, Askjaer P (2012). Dissection of the NUP107 nuclear pore subcomplex reveals a novel interaction with spindle assembly checkpoint protein MAD1 in Caenorhabditis elegans. Mol Biol Cell 23, 930–944.
Rose L, Gönczy P (2014). Polarity establishment, asymmetric division and segregation of fate determinants in early C. elegans embryos. WormBook 2014(Dec 30), 1–43.
Salina D, Bodoor K, Eckley DM, Schroer TA, Rattner JB, Burke B (2002). Cytoplasmic dynein as a facilitator of nuclear envelope breakdown. Cell 108, 97–107.
Santamaria A, Wang B, Elowe S, Malik R, Zhang F, Bauer M, Schmidt A, Sillje HHW, Korner R, Nigg EA (2010). The Plk1-dependent phosphoproteome of the early mitotic spindle. Mol Cell Prot 10, M110.004457.
Schooley A, Vollmer B, Antonin W (2012). Building a nuclear envelope at the end of mitosis: coordinating membrane reorganization, nuclear pore complex assembly, and chromatin de-condensation. Chromosoma 121, 539–554.
Solc P, Kitajima TS, Yoshida S, Brzakova A, Kaido M, Baran V, Mayer A, Samalova P, Motlik J, Ellenberg J (2015). Multiple requirements of PLK1 during mouse oocyte maturation. PLoS One 10, e0116783.
Strome S, Powers J, Dunn M, Reese K, Malone CJ, White J, Seydoux G, Saxton W (2001). Spindle dynamics and the role of gamma-tubulin in early Caenorhabditis elegans embryos. Mol Biol Cell 12, 1751–1764.
Strome S, Wood WB (1983). Generation of asymmetry and segregation of germ-line granules in early C. elegans embryos. Cell 35, 15–25.
Sumara I, Giménez-Abián JF, Gerlich D, Hirota T, Kraft C, la Torre de C, Ellenberg J, Peters JM (2004). Roles of polo-like kinase 1 in the assembly of functional mitotic spindles. Curr Biol 14, 1712–1722.
Sunkel CE, Glover DM (1988). polo, a mitotic mutant of Drosophila displaying abnormal spindle poles. J Cell Sci 89, 25–38.
Szabo SP, O'Day DH (1983). The fusion of sexual nuclei. Biol Rev Camb Philos Soc 58, 323–342.
Tapley EC, Starr DA (2013). Connecting the nucleus to the cytoskeleton by SUN. Curr Opin Cell Biol 25, 57–62.
Timmons L, Court DL, Fire A (2001). Ingestion of bacterially expressed dsRNAs can produce specific and potent genetic interference in Caenorhabditis elegans. Gene 263, 103–112.
Tong C, Fan HY, Lian L, Li SW, Chen DY, Schatten H, Sun QY (2002). Polo-like kinase-1 is a pivotal regulator of microtubule assembly during mouse oocyte meiotic maturation, fertilization, and early embryonic mitosis. Biol Reprod 67, 546–554.
van der Heijden GW, van den Berg IM, Baart EB, Derijck AAHA, Martini E, de Boer P (2009). Parental origin of chromatin in human monopronuclear zygotes revealed by asymmetric histone methylation patterns, differs between IVF and ICSI. Mol Reprod Dev 76, 101–108.
van der Voet M, Lorson MA, Srinivasan DG, Bennett KL, van den Heuvel S (2009). C. elegans mitotic cyclins have distinct as well as overlapping functions in chromosome segregation. Cell Cycle 8, 4091–4102.
Walters AD, Bommakanti A, Cohen-Fix O (2012). Shaping the nucleus: factors and forces. J Cell Biochem 113, 2813–2821.
Watanabe N, Sekine T, Takagi M, Iwasaki J, Imamoto N, Kawasaki H, Osada H (2009). Deficiency in chromosome congression by the inhibition of Plk1 polo box domain-dependent recognition. J Biol Chem 284, 2344-2353.
Zamboni L, Bell J, Baca M, Mishell DR (1966). A penetrated human ovum studied by electron microscopy. Nature 210, 1373–1375.
Zamboni L, Chakraborty J, Smith DM (1972). First cleavage division of the mouse zygot. An ultrastructural study. Biol Reprod 7, 170–193.